

**Field and modelling investigations of fresh-water plume behaviour
in response to infrequent high-precipitation events, Sydney
Estuary, Australia**

Author

Lee, Serena B, Birch, Gavin F, Lemckert, Charles J

Published

2011

Journal Title

Estuarine, Coastal and Shelf Science

DOI

[10.1016/j.ecss.2011.01.013](https://doi.org/10.1016/j.ecss.2011.01.013)

Rights statement

© 2011 Elsevier. This is the author-manuscript version of this paper. Reproduced in accordance with the copyright policy of the publisher. Please refer to the journal's website for access to the definitive, published version.

Downloaded from

<http://hdl.handle.net/10072/42650>

Griffith Research Online

<https://research-repository.griffith.edu.au>

Submitted to the Journal of Estuarine and Coastal Shelf Science

Field and modelling investigations of fresh-water plume behaviour in response to infrequent high-precipitation events, Sydney Estuary, Australia.

Serena B. Lee _A, Gavin F. Birch _A and Charles Lemckert _B

A: Environmental Geology Group, School of Geosciences, The University of Sydney, NSW, Australia

Postal address: Madsen Bldg (F09), The University of Sydney, NSW, 2006 Australia.

Phone no's: +612 9036 6532, +612 93512921

Fax no's: +612 9036 6588, +612 9351 0184

Email addresses: Serena.lee@usyd.edu.au, Gavin.birch@sydney.edu.au

B: Griffith School of Engineering, Griffith University, QLD, Australia

Postal address: Griffith School of Engineering, Gold Coast Campus, Griffith University, QLD, 4222, Australia

Phone no: +617 5552 8574

Fax no: +617 5552 8065

Email address: C.lemckert@griffith.edu.au

Abstract words: 321

Text words: 7,921

References: 1,258

Corresponding author. Email: serena.lee@usyd.edu.au

Key words: Estuary, high precipitation, fresh-water plume, stratification, salinity, hydrodynamic model

Abstract

Runoff from the urban environment is a major contributor of non-point source contamination for many estuaries, yet the ultimate fate of this stormwater within the estuary is frequently unknown in detail. The relationship between catchment rainfall and estuarine response within the Sydney Estuary (Australia) was investigated in the present study. A verified hydrodynamic model (Environmental Fluid Dynamics Computer Code) was utilised in concert with measured salinity data and rainfall measurements to determine the relationship between rainfall and discharge to the estuary, with particular attention being paid to a significant high precipitation event. A simplified rational method for calculating runoff based upon daily rainfall, subcatchment area and runoff coefficients was found to replicate discharge into the estuary associated with the monitored event. Determining fresh-water supply based upon estuary conditions is a novel technique which may assist those researching systems where field-measured runoff data are not available and where minor field measured information on catchment characteristics are obtainable.

The study concluded that since the monitored fresh-water plume broke down within the estuary, contaminants associated with stormwater runoff due to high precipitation events (daily rainfall > 50mm) were retained within the system for a longer period than was previously recognised.

1. Introduction

Estuaries are highly valued regions both economically and biologically and their shores often the site of large conurbations. Based upon estimates of annual primary production, estuaries are among the most productive of all ecosystems (Schlesinger, 1997). Contamination associated with urban activities may adversely impact on the health and productivity of organisms reliant on estuarine systems. Improved understanding of the relationship between urbanised catchments and estuary health would assist better management of the estuarine environment. Whilst point sources of pollution may be identified and practices implemented to remove any future threat these pose on the environment, non-point sources of pollution present more of challenge for management.

The Sydney estuary around which the urban hub of Sydney has developed, plays a part in everyday life for many Sydneysiders with multiple uses as a transport corridor and recreational playground. Previously, the estuary had an important

industrial role and the foreshores were home to a variety of industrial activities, including chemical and paint factories, power stations, slaughterhouses, refineries, shipping and cargo wharfs and naval facilities. Most of these activities have been relocated; still legacy contaminated sediment remains on the estuary bed. The catchment is highly urbanised (86%) and currently, the major source of estuarine contamination is via stormwater pollution (Birch and Taylor 2000), which continues to supply contaminants to the water body.

The rainfall regime in the Sydney area is characterised by generally dry conditions punctuated by infrequent, high-precipitation events (rainfall > 50mm/day). Under dry-weather conditions the estuary is well-mixed and contaminants associated with stormwater runoff deposit close to discharge points becoming permanently trapped in estuary embayments. Runoff from the catchment increases rapidly during high-precipitation events and on reaching the waterbody forms a buoyant layer above saline estuarine waters. Under these conditions, contaminants associated with stormwater runoff may migrate beyond off-channel embayments and depending on the intensity of the storm, the plume may reach the main estuary channel even exiting the estuary mouth (Birch and Taylor, 2004). The ultimate fate of contaminants associated with fresh-water plumes generated under these conditions is largely unknown.

Prior to the present study, minor research had been conducted to describe fresh-water plume behaviour in the Sydney Estuary. Wolanski (1977) described the behaviour of buoyant fresh-water plumes in the upper 4 km of the estuary from the headwaters to the eastern side of Homebush Bay (Figure 1). The fresh-water plume he described was short-lived and moved down-estuary on top of the marine water on the ebb tide remaining largely stationary during the incoming tide. Some fresh water migrated down-estuary possibly flushing into the lower estuary (Sydney Harbour). It was found initially that tidal turbulence mainly affected fresh water at the fresh/saline water interface where fresh water became entrained downward through the water column. Approximately 5 days following the high-precipitation event, tidal turbulence had significantly mixed the plume causing it to disperse (Wolanski, 1977). Taylor (2000) also documented the presence of a fresh-water plume in Iron Cove, an off-channel embayment on the southern shoreline of the estuary. Taylor (2000) found that following a high-precipitation event, sediment supply to the bed (i.e. settling) of the embayment was suppressed. Under these conditions terrigenous sediment was

retained in the upper, fresh-water plume and was transported beyond the embayment and into the main estuary channel.

The first objective of the present study was to extend the description of fresh-water plume behaviour to describe salinity distributions throughout the entire system from the headwaters and embayments to the estuary mouth following a high-precipitation event. To monitor and describe the observed fresh-water plume, salinity profiles were obtained from between 26 and 34 sites over 3 days following a high-precipitation event– thus recording temporal and spatial changes in fresh water distribution throughout the estuary. The average return interval of the monitored event was 1 year. Secondly, a hydrodynamic model, which could be used to replicate the generation of fresh-water plumes in the estuary, was constructed and validated. The hydrodynamic model was verified with respect to water level, cross-sectional discharge and current velocity. Given the lack of field data relating to fresh water runoff from the catchment, the verified hydrodynamic model was used to determine the appropriate rainfall/runoff relationship capable of replicating the measured response in the estuary to the high-precipitation event. Lastly, utilising the hydrodynamic model, plume break down and the time taken for the system to return to well-mixed (quiescent) conditions was predicted.

This study is the first to document three dimensional salinity distributions throughout the entire Sydney Estuary in response to a high-precipitation event and is the first attempt to provide a verified model of fresh-water plume behaviour throughout the whole system. The model will provide valuable information on the fate of stormwater and associated contaminants supplied from the catchment and will be a valuable aid in formulating strategies for management of this iconic waterway.

2. Materials and Methods

2.1 Site Description

The Sydney Estuary is a microtidal (maximum tidal range = 2.1m) drowned river valley (Roy, 1983) with a meandering main channel approximately 30 km in length (Figure 1). Sydney Harbour and Port Jackson are only parts of the estuary (McLoughlin, 2000a; Birch and Murray, 2009). In the present work we refer to the ‘Sydney Estuary’, which includes all submerged areas to low water and excludes the northern arm of the estuary - Middle Harbour – which acts hydrodynamically as a

separate entity. The waterway covers approximately 50 km², and drains a highly urbanised (86%) catchment approximately 500 km² (Birch and Taylor, 2004).

The waterway is geometrically complex and bathymetry is irregular (1 to 46m deep with a mean water depth of 13m). The Parramatta, Duck and Lane Cove Rivers are the largest tributaries of the system (Figure 1). During dry weather conditions fresh water discharge is low (< 0.1 m³/s at all discharge locations) (Rochford, 2008; Birch and Rochford, 2010) and salinity throughout the estuary is vertically homogeneous (Hatje, 2001a). Both low fresh-water discharge and tidal turbulence contribute to well-mixed estuarine conditions with salinity ranging from 27 PSU at the headwaters to 35 PSU at the estuary mouth in the absence of precipitation. Flushing rates throughout the estuary differ significantly with estimated flushing rates reaching 225 days (Das, et al., 2000).

Sydney has a temperate, coastal climate (Cruishank 2006) with mean daily temperatures from 16.3 °C to 25.9 °C (Bureau of Meteorology (BoM) 2010). The rainfall pattern is erratic and spatially variable. Average mean monthly rainfall between the years 1859 and 2010 ranged from a minimum of 69.1 mm in September to a maximum of 130.6 mm in June. The mean number of days where rainfall exceeded 1mm ranged from 7.2 days in August to 9.8 days in March over this period (BoM 2010). Presently there are no published data measuring runoff rates during and following high precipitation events to the estuary aside from a study limited to Iron Cove (Figure 1), an off-channel embayment on the southern foreshores of the estuary (Davies 2010).

2.2 Rainfall Distribution

To describe the spatial and temporal variations in rainfall across the catchment associated with the monitored high precipitation event rainfall distribution was mapped using daily rainfall data collected by the Bureau of Meteorology, from 26 locations within the catchment (see Figure 1) and an additional 8 sites within 5 km of catchment boundary. A linear relationship was assumed for spatial data interpolation using the ArcGIS mapping software. These maps give an indication of the intensity and duration of the high precipitation event across all subcatchments. Each high precipitation event is unique and recording rainfall data and measuring related fresh-water plume development, allows relationships between catchment rainfall distribution and corresponding estuary salinity distributions to be identified.

2.3 Field measurements of fresh-water plume behaviour

To record the structure of the water column within various parts of the estuary a Conductivity Temperature and Depth (CTD) probe, set to record every 5 seconds (YSI Model 6920V2 with a YSI 6136 optical turbidity probe) was manually lowered from the water surface to the estuary bed. CTD measurements were collected on the 25th, 26th and 28th of April 2007, one, two and four days following the day of heavy rainfall (on the 24th of April 2007). Due to limited equipment and the time taken to cover the estuary, data were manually collected from each site once a day. Site locations are displayed in Figure 2a.

Maps of surface water salinity were generated using ArcGIS mapping software from data collected from between 24 and 34 sites, 0.5m below the water surface for each day of monitoring. Estuary profiles describing vertical salinity distributions along the axis of the estuary were generated from data collected down the water column at 15 to 17 main channel sites for the three days of monitoring. A linear relationship was assumed between the data points and for the surface water salinity maps, data were bounded by a polyline representing the Sydney estuary shoreline.

2.4 Cross-sectional discharge and current speed measurements

Acoustic Doppler Current Profile (ADCP) data were collected across the main estuary channel in the lower, central and upper estuary, as well as across Iron Cove, Homebush Bay and Lane Cove River for model verification. A 1200 kHz RD Instruments Workhorse ADCP was employed for all ADCP measurements. Bottom tracking was implemented to account for boat speed (speeds ~ 1-2 m/s) and horizontal ensemble lengths ranged between ~ 0.8 and 2m. In the vertical direction, 0.5m bins were applied. ADCP measurements were limited at the very top and bottom of the water column due to ADCP blanking - 1.2m and 1m respectively.

ADCP data were obtained for three days of a King Spring tide cycle (Highest Astronomical Tide) in February 2007 from 9 different estuary cross-sections and four days of a Spring tide cycle in January 2008 from 2 cross-sections within the Iron Cove embayment. During the February 2007 study, measurements along each transect were collected during ebb tide (tidal range = 1.73m, 1.82m, 1.8m and 1.43m for the 17th, 18th, 19th and 21st of February, respectively) in daylight hours. In the course of the January 2008 field study numerous transects were conducted over a four-day period

across two sections of the embayment. The time lapse between consecutive measurements at each cross-section was approximately one hour. Transect locations are displayed in Figure 2a labelled T₁ to T₉.

All ADCP data were interpreted using WinRiver II software (obtained from Teledyne R D Instruments). A full description of the post processor is contained in the WinRiver II Users Guide (Teledyne RD Instruments, 2007). Discharge and current velocity through unmeasured sections of the water column was estimated by the WinRiver II post-processor by instituting a power law (Chen, 1991) with a power curve coefficient = 0.1667. The influence of anthropogenic activities, i.e. wakes from ferries, rivercats, barges, jet boats, shipping and large recreational vessels, were removed manually.

Data from a bottom-mounted ADCP located near Balls Head in the main channel of the central estuary (Fig. 2a) were obtained from the Sydney Harbour Ports Authority. This dataset provided a time series for the month of February 2007 of average current speed recorded every minute in the upper 12m of the water column at this location

2.5 Model description

A three-dimensional hydrodynamic computational model was used to replicate flow patterns within the estuary. The model selected for this purpose was the Environmental Fluid Dynamics Computer Code (EFDC) developed by Hamrick at the Virginian Institute of Marine Science. Hamrick (1992) documents the computational and theoretical basis for the model. Detailed descriptions of model equations and assumptions are provided in the EFDC User Manual (Users Manual for the Environmental Fluid Dynamics Computer Code, J.M. Hamrick 1996). Pre- and post-processing was conducted using EFDC-Explorer (Craig, 2005).

EFDC has been applied to numerous surface water systems throughout USA including Chesapeake Bay (Hamrick, 1994a), the Indian River Lagoon (Moustafa and Hamrick, 1994, Moustafa, et. al., 1995) Lake Okeechobee in Florida, Peconic Bay in New York (Tetra Tech, 1999), St Louis Bay, Mississippi (Liu, et. al., 2008) and the Palmico River Estuary (Xu, et. al., 2008). Additionally EFDC has been utilised for hydrodynamic and water quality studies in the Asia Pacific, including the Yellow Sea between mainland China and the Korean Peninsula (Luo & Li, 2009), Kwang-Yang Bay, Korea (Park et al, 2005) and the Tasman/Golden Bay system in New Zealand

(Tuckey, et al., 2006). The modelling package is capable of simulating one or multi-dimensional flow, transport and bio-geochemical processes in a variety of aquatic systems and has been successfully applied to lakes, rivers, reservoirs, estuaries, coastal lagoons, bays and wetlands (Hamrick, 1992b; Zarillo and Surak, 1995; Yang, 1996; Kuo et al., 1996; Zarillo, 1998; Shen et al., 1999; Ji et al., 2000; Lin and Kuo, 2003; Shen and Haas, 2004; Park et al., 2005; Shen and Lin, 2006; Lin et al., 2007, 2008a; Xu et al., 2008; Liu et al., 2009; Huang et al., 2009).

EFDC has the capacity to model eutrophication processes, sediment transport and fate of dissolved and particulate phases of contaminants. In the present study only applications simulating hydrodynamics, salinity and temperature were utilised. Many aspects of the computational schemes in EFDC are equivalent to the Princeton Ocean Model (POM) developed by Blumberg and Mellor (Blumberg and Mellor, 1987). The EFDC model domain is described using curvilinear orthogonal horizontal coordinates and sigma vertical coordinates. The equations of momentum are solved on a staggered or C grid using second-order accurate spatial finite differencing. Time integration is conducted using a second-order accurate three-time level, finite difference scheme. An internal-external mode splitting procedure is implemented to separate the baroclinic mode from the barotropic mode. The semi-implicit external mode solution computes the two-dimensional surface elevation field simultaneously through the application of a pre-conditioned conjugate gradient procedure. Calculation of the depth-averaged barotropic velocities using the new surface elevation field completes the external solution. The semi-implicit external solution allows large time steps constrained only by the stability criteria of the explicit central difference or higher order upwind advection scheme to be utilised in model simulations. At the same time step as the external solution, the internal momentum equation of the model is implicit with respect to vertical diffusion and is expressed in terms of the velocity shear and vertical profile of the shear stress. Periodic insertion of a second-order accurate two-time-level trapezoidal step controls time splitting in the three-time-level scheme.

By implementing the Mellor-Yamada level 2.5 turbulence closure scheme as modified by Galperin et al. (1988) for the two turbulence parameter transport equations, EFDC also solves the dynamically coupled transport equations for turbulence length scale, turbulent kinetic energy, salinity and temperature.

A Lagrangian particle transport transformation scheme and an arbitrary number of Eulerian transport-transformation equations for dissolved and suspended

materials are also incorporated within the EFDC model package. Wetting and drying is simulated using a mass conservation scheme.

2.5.1 Model Set Up

The RGFGrid software developed by Delft Hydraulics (now Deltares) was utilised for grid construction. Care was taken to include all tributaries and embayments in the model domain whilst accurately following the meandering path of the main estuary channel. The horizontal grid consists of 12309 cells with an average cell size of 70m x 62m. Up to 15 vertical sigma layers were utilised.

Model bathymetry was based upon GeoSwath data collected within the Sydney estuary by GeoAcoustics for the Shallow Water Survey, 2003. Grid cells located adjacent to headlands or islands were manually edited using bathymetric survey maps as a reference.

The hydrodynamic behaviour of the Sydney Estuary is driven by tidal forcing at the mouth. To replicate this behaviour an open boundary was instituted incorporating the grid cells across the mouth (Fig. 2b) and a file describing predicted water level due to tides at Fort Denison (Fig 2b) uniformly applied to the boundary. The Foreman Tide program (Foreman, 1977) was used to generate the water level file. Given that the tidal lag for the entire estuary is approximately 10 minutes, using data from Fort Denison to represent estuary mouth water levels was deemed appropriate.

To simulate wetting and drying, dry and wet depths were set to 0.07m and 0.11m, respectively with a dry step of 20. The model simulation time-step was set to 2 seconds.

In the present study, the effects of sediment transport were ignored and the bed simply represented as a solid surface with a uniform bed roughness. Much of the estuary is mantled in fine sediment ($<62.5 \mu\text{m}$). Physical bedforms are absent in off channel areas of the estuary due to low ambient energy and minor tidal currents, only bioturbation (biological bed disturbance, mainly callianassid shrimp) is observed. Mounds from biological activity approximately 2cm high were observed by Taylor (2000). Bedforms are likely to be present in the lower estuary region near the mouth, however presently there are no published data from which to base roughness estimates in this region. Tidal currents have scoured the bed along most of the main estuary channel in the central estuary region. Based upon the information available, bed

roughness was uniformly set to 2cm across the model domain to account for the presence of burrows and worm casts.

Atmospheric conditions were simulated using half-hourly wind velocity data collected within the lower estuary at Fort Denison (BoM) (Figure 2c.) and applied uniformly to the entire grid. This was deemed appropriate for the present study since winds were light to moderate for the duration of the event. The effects of sheltering by local topography were not addressed in the present study and additional atmospheric data (i.e. radiation) were not available. For future studies addressing events where winds velocities were more significant (consistently >20 knots) a spatially varying wind file will be applied to the model grid.

Wave activity associated with ocean swells is typically limited to the lower estuary within 4 km of the mouth. Consequently the influence of ocean waves is not addressed in the present study. Local wind wave amplitudes are typically less than 40 cm during periods of high (> 30 knot) wind (Birch and O'Hea, 2007). Presently, the EFDC model framework accounts for action of wind by considering the effect of wind stress at the free surface. In future, a wind-wave model (i.e. SWAN) may be linked to the EFDC model of the estuary.

Initial conditions for salinity were based on measurements collected during quiescent conditions (Hatje et al. 2001a). During quiescent periods, water temperature typically varied by only a few degrees in horizontal and vertical directions. Water temperature recorded at Fort Denison during the period of the present investigation was approximately 22 °C. This value was used to create the initial water temperature file for the entire grid. At the flow boundaries water temperature was made equal to the mean ambient air temperature recorded on the 24th of April 2007, the day of heaviest rain.

Fresh water discharge was simulated by applying a number of point-discharges to the model domain. Flow boundary positions, representing tributaries and stormwater outlets, were identified from estuary maps, aerial photographs and visual observations. Field-measured base-flow data were applied to replicate fresh-water supply during quiescent conditions (Rochford, 2008; Birch and Rochford, 2010). The Model for Urban Stormwater Improvement Conceptualisation (MUSIC) was used to predict base-flow for subcatchments where field measured data were not available (Rochford, 2008; Birch and Rochford, 2010).

An empirical method used successfully in local studies (Rochford, 2008; Birch and Rochford, 2010; Davis, 2010; Davis and Birch, in press) was utilised to calculate runoff rates associated with high-precipitation events. A simplified version of the Rational Method for calculating discharge is provided in Equation 1

Eqn 1

$$Q = \phi i A$$

Where:

Q is the daily runoff rate in m^3/s ,

ϕ is the runoff coefficient (R.C)

i is the average rainfall intensity (m/s)

A is the subcatchment area (m^2)

As previously mentioned, rainfall patterns throughout the catchment can be spatially and temporally variable. Davis (2010) reported high spatial variability in rainfall measurements collected within a single subcatchment (Iron Cove, Sydney, Australia) over several different rainfall events from sites 4 km apart. In past studies, annual average rainfall measurements at sites across the catchment have been used to construct precipitation scaling factors for the entire Sydney catchment (Cruickshank, 2006; Birch and Cruickshank, 2010; Rochford 2008; Birch and Rochford, 2010). The scaling method proved useful in the construction of long term (decadal) predictive models yet this approach is inappropriate for determining rainfall in subcatchments for particular high-precipitation events for specific days of the year which is the primary interest of the present study. For this reason measured rainfall obtained from gauges within individual subcatchments were used to calculate runoff rates. For subcatchments where no rain gauge measurements were available, rainfall data were taken from the nearest rain gauge or gauges (typically within 3km of subcatchment boundaries). Rain gauge locations within the catchment are displayed in Figure 1. The effects of fluctuations in storm intensity on scales smaller than 24 hours were not considered since higher resolution rainfall data were not available for the majority of rain gauges. Rainfall intensity was assumed to be constant over a 24-hour period, thus from equation 1, $i = \text{Daily Rainfall (m)}/86400(\text{s})$.

R.C data were obtained for 19 of the 70 estuary subcatchments from Ferguson et al. (1995) and AWT Ensign (1996). The use of constant R.Cs to determine runoff rates in urban catchments has been challenged over the past decade. Bucciu and Paoletti (2000) showed that rather than being a constant value, ϕ (from equation 2) is variable, even for highly-urbanised catchments where impervious area was greater than 90%. Davis (2010) revealed an incremental relationship between rainfall and runoff with the R.C varying from 0.35 for rainfall events $< 6\text{mm/day}$ to 0.97 for rainfall events $> 20\text{mm/day}$ within the Iron Cove Creek subcatchment. The lack of runoff measurements from estuary tributaries, replicating stormwater discharge remains a major hurdle in accurately modelling fresh-water plume behaviour. In the absence of field-measured data, or a verified catchment runoff model for the system, four rainfall/runoff scenarios have been assessed by comparing modelled salinity distributions generated under the different rainfall/runoff regimes with field data collected throughout the estuary.

2.5.2 Model Calibration

The initial parameters used for bottom roughness (2cm), horizontal momentum diffusivity (HMD) coefficient ($0.2\text{ m}^2/\text{s}$), vertical eddy viscosity ($1 \times 10^{-8}\text{ m}^2/\text{s}$) and vertical molecular diffusivity ($1 \times 10^{-6}\text{ m}^2/\text{s}$) generated model results for water level, cross-sectional discharge and water velocity which agreed closely with field measured data. To test the impact of altering the bottom roughness a variable bed was created ($50\text{cm} < \text{bottom roughness} < 2\text{cm}$) increasing the bed roughness up to 50cm in the lower estuary in the 4km area near the estuary mouth. Comparison of discharge data over a seven day period between the uniform roughness model and the variable roughness model generated RMSE = $63\text{ m}^3/\text{s}$ for T9 (Figure 2a) in the lower estuary, $30\text{ m}^3/\text{s}$ for T8 in the central estuary, reducing to $1.7\text{ m}^3/\text{s}$ for T2 in the upper estuary. Comparison of water level files at Fort Denison gave an RMSE of 1cm. The higher bed roughness applied in the lower estuary affected discharge and current speeds in this region, however due to the lack of published data relating to bed roughness the uniform roughness model was utilised in the present study given the differences were not significant throughout most of the system.

Altering the vertical eddy viscosity by 3 orders of magnitude had no measurable effect on water level, discharge, velocity and salinity predictions.

Similarly, sensitivity tests applying HMD values between $0.1 \text{ m}^2/\text{s}$ and $0.25 \text{ m}^2/\text{s}$ revealed little impact on modelled water velocity with predicted velocities varying by less than 1 cm/s . Altering the HMD by up to a factor of 2.5 resulted in small changes in predicted salinity (≤ 1).

Changing the vertical molecular diffusivity (VMD) by up to 4 orders of magnitude had no effect on predicted water levels, cross-sectional discharge and current velocities but predicted salinities were altered. Given that there is no long term monitoring of runoff and estuary response, calibration was tested by running the model using an initial salinity file generated from data collected throughout the estuary following high rainfall when stratification was already present.

Initial salinity conditions for the VMD calibration model runs were generated from vertical salinity profiles measured throughout the system on the 25th of April 2007 (the day after highest rainfall). The VMD was altered from $1 \times 10^{-9} \text{ m}^2/\text{s}$ to $1 \times 10^{-4} \text{ m}^2/\text{s}$ and predicted salinities from each run compared with field data collected on the 26th and 28th of April, 2007. The model run commenced at 12pm on the 25th of April and it was assumed that the majority of rain had fallen prior to this time. Consequently it was assumed that baseflow conditions represented runoff at the flow boundaries for the VMD calibration model run.

Model results showed closest agreement to salinity data in the horizontal and vertical directions when vertical molecular diffusivity (VMD) values $\leq 1 \times 10^{-8} \text{ m}^2/\text{s}$ were applied. Stratification was not well represented by the higher VMD values and results from these model runs predicted more mixing in the vertical direction than was measured in the field.

$\text{VMD} = 1 \times 10^{-8} \text{ m}^2/\text{s}$ was deemed appropriate for further modelling investigations addressing fresh-water plume behaviour in the estuary. This value was of a similar order of magnitude to the vertical eddy diffusivity determined for the Swan River estuary ($6.5 \times 10^{-8} \text{ m}^2/\text{s}$) from direct measurements (Etemad-Shahidi & Imberger, 2005). In future it would be prudent to readdress the calibration of the VMD when longer-term field data relating measured runoff rates to measured estuarine conditions becomes available.

2.5.3 Model Verification

The model generated accurate results for water level, discharge, velocity (Fig. 3) and salinity despite the small amount of data available for calibration. Turning base-flow on and off did not affect results achieved for these parameters. This is likely due to the low base-flow rates associated with quiescent conditions.

2.5.3.1 Water Level

A comparison of measured water levels from Fort Denison and the modelled water level at the corresponding grid cell over a 15-day period, from the 10th to the 25th of February 2007 is displayed in Figure 3a. Root mean square error (RMSE) = 0.09m.

2.5.3.2 Cross-sectional Discharge

Flux lines were constructed across grid cells closely corresponding to ADCP field Transect locations. Two model runs were conducted. The first was from 1st - 28th of February 2007 and the second from 1st - 31st of January 2008, to incorporate periods when ADCP field measurements were obtained. Modelled and measured discharge data are displayed concurrently in Figures 3b and 3c.

The RMSE for individual transects ranged from 19 m³/s for T₂ to 218 m³/s for T₈ and the average RMSE for all transects = 112 m³/s. The highest degree of disagreement between measured and modelled cross-sectional discharge data was noticed for Transects crossing the main channel in the lower and central estuary (T₇, T₈ and T₉). All three transects cross busy transport corridors making data collection problematic. The ADCP occasionally lifted out of the water column due to large wake waves associated with shipping and public transport vessels causing data to be lost. For all three transects the model predicted higher discharges than were measured by the instrument during maximum semi-diurnal ebb velocities (Figure 3). This is likely due to data gaps incurred during field investigations at these locations. Accounting for the difficulties encountered during field investigations the level of agreement is considered adequate and water flow throughout the entire system is represented with sufficient accuracy.

2.5.3.3 Current Velocity

Figure 3d displays the ADCP current speed data recorded from the upper 12m of the water column measured by the bottom-mounted ADCP located near Balls Head (instrument location displayed in Fig. 2a). A first-order Butterworth filter (cut-off

frequency = 0.167 Hz) was applied to the raw ADCP data to reduce some of the noise generated by anthropogenic activities associated with shipping, etc.

Data extracted from the grid cell encompassing the ADCP location is also displayed. The model run used two vertical layers constructed such that thickness of the top layer at the grid cell corresponding to the ADCP site equalled 12m at mid tide.

Modelled current speeds were within 5cm of measured current speed data 88% of the time and RMSE = 3.2 cm/s or 28% with respect to the mean velocity reported by the ADCP.

Depth-averaged current speed data obtained from ADCP transect measurements in the upper, central and lower estuary were compared to modelled current speeds across transects to determine the accuracy with which the model represented the hydrodynamic conditions present throughout the estuary. Measured current speed data were averaged over the distance corresponding to the appropriate grid cell distance and compared with depth-averaged current speeds reported by the model for the time closest to that of measurement. Transects used for current velocity comparisons were Transects 2, 3, 5, 6, 7, 8 and 9. Examples comparing modelled and measured current speed data across 3 different Transects during maximum ebb tide velocity are displayed in Figures 3e and 3f.

Agreement between predicted and measured current speed throughout the system is summarised in Table 1. Difference between modelled and measured current speeds throughout the system were less than +/-5cm/s, 88% of the time and RMSE = 3.1 cm/s. These results demonstrate that the hydrodynamic model is capable of replicating currents throughout the entire estuary.

2.6 Modelling Investigations of the April 2007 High-Precipitation Event.

Four different rainfall runoff scenarios were used to determine the potential runoff to the estuary resulting from the April 2007 high precipitation event. These scenarios are described below:

Scenario 1 – Runoff rates were calculated using Equation 2, for the 19 subcatchments for which R.C data ($0.3 \leq \phi \leq 0.77$) were available (Figure 2b). Runoff from these subcatchments (Figure. 2b) flowed into six river systems, i. e. Parramatta, Duck and Lane Cove Rivers, Haslam, Powell and Iron Cove Creeks and cover 77% of

the total catchment. Eleven flow boundaries were instituted in the model domain to simulate stormwater runoff flowing into Parramatta, Duck and Lane Cove Rivers. A flow boundary was also instituted where Iron Cove Creek discharges into Iron Cove and 3 flow boundaries were implemented near the bay end of Homebush Bay to simulate fresh-water discharge from Haslams and Powells Creeks. Stormwater discharges from the additional 51 subcatchments were not simulated in this scenario.

Scenario 2 – Scenario 1 discharges were augmented with runoff from the remaining 51 subcatchments for which R.C data were not available. Twenty eight additional flow boundaries were instituted across the model domain replicating discharge from these subcatchments and runoff rates were calculated using Equation 2, $\phi = 0.3$ (the lowest reported R.C, equivalent to that for the Parramatta River subcatchments). Locations of the Scenario 2 flow boundaries are shown on the model grid displayed in Figure 2b.

Scenario 3 – The implications arising from variable R.Cs due to catchment surface saturation were addressed by the regime implemented in this scenario. As rainfall increased the pervious surfaces became saturated and the entire subcatchment began to act as an impervious surface. Runoff rates for all subcatchments were calculated using R.Cs determined by Davis (2010) for the Iron Cove Creek subcatchment assuming that these reflected R.C's for the entire catchment. R.Cs increased incrementally in three stages. For the first 6mm/day of rain, $\phi = 0.35$. For rainfall between 6 and 20 mm/day $\phi = 0.567$ and when rainfall exceeded 20 mm/day $\phi = 0.97$. R.C remained equal to 0.97 the day following rainfall > 20 mm, after which lower ϕ were applied dependant upon rainfall. Runoff rates were individually calculated for each subcatchment and applied to the 45 flow boundary locations used in Scenario 2.

Scenario 4 – In this regime the reliability of using the subcatchment percent impervious area (I.A) as a proxy for the runoff coefficient was tested. This scenario assumed that runoff was only generated by the impervious areas and that 100% of rain falling on these surfaces contributes to runoff. Further that rain falling on all pervious surfaces was absorbed by the catchment and did not contribute to runoff to the estuary. The I.A was applied to Equation 2 in place of runoff coefficients to calculate runoff rates for the 45 flow boundaries representing fresh-water discharge to the estuary. I.A varied from 0.62 to 0.4 throughout the catchment.

The four schemes described covered the entire range of possible rainfall/runoff relationships from the scheme generating the minimum runoff (Scenario 1) to that generating the highest runoff volume (Scenario 3). Model runs applying the different rainfall/runoff regimes will be referred to as Scenario 1, Scenario 2, Scenario 3 and Scenario 4.

Fifteen vertical water layers were instituted and simulations were conducted from the 20th to the 29th of April 2007. Predicted salinity data were extracted at times closest to that of field data collection (within 15 minutes) at each location and the flow boundary conditions which achieved the closest agreement with field data were identified.

Following the determination of the appropriate flow boundary conditions the computation period was extended, assuming no further rain fell in the catchment, in order to predict the time taken for the system to return to quiescent conditions.

3 Results

3.1 Catchment Conditions, Rainfall Distribution

Figure 4 shows temporal (daily) and spatial rainfall patterns associated with the April 2007 high-precipitation event. The rain event was short-lived lasting three days (23rd to 25th) before abating. Initially (23rd), rainfall was more intense near the coast, but rainfall was most intense the following day when the storm range extended and rainfall increased over the entire catchment. On the third day (25th), the storm veered north.

3.2 Estuary Conditions

3.2.1 Salinity data

Results from the CTD instrument revealed a fresh-water plume was generated primarily in response to rainfall on the 24th of April 2007. Salinity was lowest at the top of the water column at all sites on all three days (25th, 26th and 28th) of monitoring. The fresh water influence was most pronounced in the upper estuary, and in the Lane Cove River.

Salinity profiles collected in the main estuary channel upstream of Site 26 (the Gladesville Bridge) on the 25th of April showed clear stratification at deeper water sites. By contrast where water depth was less than 6m, the salinity gradient was

approximately linear, suggesting more interaction between fresh and marine waters in shallower areas.

Initially (25th of April), lower salinities were limited to the upper ~2m of the water column. Results one and three days later indicated that fresh water became entrained down the water column mixing with the underlying marine water (Fig 6c and 6e). The front ($28 < \text{salinity} < 31.5$) also migrated approximately 1.5 km further down-estuary over this period.

3.2.2. Model Results

Agreement between modelled and measured estuary salinity for all four rainfall/runoff scenarios are presented in Table 2. Figure 7 displays predicted vertical salinity profiles for 3 estuary sites (Site 23, 3 and 29, locations shown in Figure 2a), along with the corresponding field salinity profiles from these locations.

From Table 2 and Figure 7 it can be seen that the regimes using reported runoff coefficients to calculate runoff rates (Scenarios 1 and 2), most accurately reproduced monitored fresh-water plume behaviour for this event. When saturation of the catchment was considered in determining runoff rates (Scenario 3) fresh water was over-supplied to the estuary (Figure 7). The Scenario 4 model run achieved salinities close to those measured throughout most of the system excepting in the upper estuary where the amount of fresh-water was over-predicted (Figure 7).

Figure 5 displays the agreement achieved between field and modelled surface water salinity based upon Scenario 2 model results for the 25th (Figure 5.b) 26th (Figure 5.d) and 28th of April 2007 (Figure 5.f). Figure 6 displays the predicted salinity profiles along the axis of the estuary (Figures 6.b, 6.d and 6.f) with corresponding field profiles are displayed alongside. Predicted plume behaviour 6, 13 and 21 days following high precipitation are displayed in Figures 6g, 6h and 6i.

Figures 5 and 6 show that Scenario 2 reproduced similar salinity distributions in both the horizontal and vertical directions as the field data. Disagreement was highest in the Lane Cove tributary (Figure 5) where predicted surface water salinity was higher than the field data by up to 12. Agreement between the modelled and measured datasets increased over time.

Model results of plume behaviour 6, 13 and 21 days following high precipitation (Figures 6g, 6h and 6i) demonstrated that fresh water mixed with the

underlying marine water inside the estuary gradually flushing from the system in a heavily diluted form ($31.5 < \text{salinity} < 35$).

In investigating the time taken for the system to return to quiescent conditions, it was assumed that the system was well-mixed once salinity variation between the top and bottom of the water column was below 2 PSU and predicted depth-averaged salinities were within 1 PSU of values reported by Hatje (2001). Model results showed that in the absence of further rainfall, the estuary took between 21 and 24 days to return to quiescent conditions following the April 2007 high-precipitation event.

4. Discussion

4.1 Catchment Conditions, Rainfall Distribution

Rainfall varied both throughout the Sydney catchment, and within individual subcatchments demonstrating the typical localised nature of precipitation in the Sydney area.

4.2 Estuary Conditions

4.2.1 Field measured salinity distributions

Results obtained for the upper estuary agree with those presented in the Wolanski study (Wolanski, 1977). The present measurements showed fresh water occupied a slightly increased portion of the water column than previously reported. This is likely due to the higher rainfall associated with this event (~50 mm/day) compared with that described in the former paper (Maximum daily rainfall = 30mm). The limited horizontal movement of the plume after the 25th of April suggests that the plume is unlikely to reach the mouth as a distinct surface-water layer given that rainfall ceased and as such any further downstream movement would have been driven by tidal processes. This supposition could not be confirmed based only upon the limited temporal field data.

4.2.2. Model Predicted Salinity Distributions

Modelling investigations showed that the incremental runoff coefficient trend observed by Davis (2010) in the Iron Cove Creek subcatchment did not accurately reproduce runoff rates for the April 2007 high precipitation event (reflected in the results obtained from Scenario 3 model results). The amount of rainfall determined by

Davies (> 20 mm/day) to cause soil saturation for the Iron Cove Creek subcatchment did not reflect the behaviour of the entire catchment in response to this event. Further research is needed to determine the conditions likely to result in saturation across the entire catchment. Soil saturation may become important when modelling events with higher daily rainfall and storm duration longer than that witnessed in the present study.

Whilst using I.A as a substitute for the runoff coefficients to determine runoff to the estuary (Scenario 4) did not produce as accurate results as those using reported runoff coefficients, the resulting salinity distributions were similar to field data throughout most of the system. This method may prove useful when determining runoff from urban environments where little catchment data is available.

The close agreement between Scenario 1 and Scenario 2 model results showed that runoff from the minor subcatchments had minimal effect on estuarine salinity.

From modelling studies it was found that the plume dispersed within the estuary. Initially fresh-water was largely contained within the upper 2m of the water there is more interaction between the plume and the underlying estuarine waters than was previously recognized. This discovery has implications for estuary managers addressing the health of the system since there is likely to be more opportunity for estuarine organisms and bottom sediment to interact with stormwater associated contaminants than had been previously acknowledged.

5. Conclusions

Estuary stratification resulting from the April 2007 high-precipitation event was short lived. Runoff volumes returned to near base-flow conditions within two days of the high-precipitation event after which time plume migration relied upon tidal forcing. Over successive tidal cycles the lower-salinity surface-water plume became entrained down the water column. Fresh water supplied to the estuary migrated out of the system in a heavily diluted state ($31.5 < \text{salinity} < 35$ PSU) due to tidal forcing and the system returned to well-mixed conditions after 3 weeks. The plume did not rapidly escape the estuary as a defined upper-fresh-water layer as was previously thought. Rather, stormwater runoff mixed with underlying estuarine water before eventually flushing from the system.

In this study, a verified hydrodynamic model proved a valuable tool to investigate estuarine response to different fresh water supply conditions. In

conjunction with modelling investigations, measured estuarine response was successfully used to determine likely catchment discharge associated with the April 2007 high-precipitation event. Using estuarine data to determine catchment discharge is a novel method which may prove useful in investigations of other systems where little data on fresh-water flows from the catchment are available.

Best estimations of runoff were determined using reported R.C data. Modelling experiments showed that if R.C data were not available, substituting subcatchment percent impervious area (I.A) for the runoff coefficient in runoff rate calculations provided a good first step toward understanding flow from the catchment in response to the high-precipitation event. The latter method may prove useful when investigating other systems where information on urban subcatchment conditions is limited.

Model results showed that soil saturation did not contribute to increased catchment runoff for this event. Further investigation is required to determine the impact of soil saturation on runoff volumes generated by other events where rainfall is higher, or storm duration longer.

The model described in the present study provides an initial step toward a better understanding of the ecosystem and estuarine response to high precipitation in the catchment and is a valuable tool which will be used for further investigations to predict transport of sediment and contaminants associated with stormwater runoff. Additionally, the model may be used to test the effectiveness of different stormwater management and remediation options, providing managing authorities with a tool to assist in the determination of effective strategies to improve estuarine health.

Acknowledgments

This study was supported by an Australian Postgraduate Award (Industry) from the Australian Research Council (No. LP0455486). Parramatta City Council on behalf of the Parramatta River Estuary Management Committee (PREMC) provided additional financial support.

The authors wish to thank the anonymous reviewers whose comments were very instructive and helpful.

The authors are grateful to The Griffith School of Engineering, Griffith University Queensland for the generous loan of the ADCP instrument and technical assistance.

Thanks to Paul M. Craig of Dynamic Solutions for training and continued technical support with the EFDC hydrodynamic model and the EFDC-Explorer Pre and Post Processor software.

Doug Treloar, Sean Garber and the team from Cardno Lawson and Treloar are thanked for provided training in modelling, land boundary construction, grid construction and additional technical advice.

We are greatly appreciative of assistance preparing equipment and participating in field trips provided by Tom Savage, David Mitchell and Marco Olmos

References

AWT Ensignt., 1996b. Stormwater monitoring project, Sydney Water Clean Waterways Unit, 1995 Report

Birch, G.F., Cruickshank, B., Davis, B., 2010. Modelling nutrient loads to Sydney estuary (Australia). *Environmental Monitoring Assessment*, 167(1-4), 333-348.

Birch, G.F., Murray, O., Johnson, I., and Wilson, A., 2009. Reclamation in Sydney Estuary, 1788-2002. *Australian Geographer*, 40/3, 347-368.

Birch, G.F., and O’Hea, L., 2007. The chemistry of suspended particulate material in a highly contaminated embayment of Port Jackson (Australia) under various meteorological conditions. *Environmental Geology*, 53, 501-516.

Birch, G.F., and Rochford, L., 2009. Stormwater metal loads to the Sydney estuary (Australia). *Environmental Modelling and Assessment*, DOI 10.1007/s10661-009-1195-z

Birch, G.F., and Taylor, S.E., 2004. Sydney Harbour and Catchment: Contaminant status of Sydney Harbour sediments: A handbook for the public and professionals. Geological Society of Australia, Environmental, Engineering and Hydrogeology Specialist Group, Sydney, 101 pp.

Blumberg, A.F., and G.L. Mellor., 1987. A description of a three-dimensional coastal ocean circulation model. In: *Three-Dimensional Coastal Ocean Models, Coastal and Estuarine Science*, Vol. 4. (Heaps, N. S., ed.) American Geophysical Union, pp. 1-19.

Chen, C.L., 1991. Unified theory on power laws for flow resistance. *Journal of Hydraulic Engineering*, 117, 371-389

Craig, P.M., 2005. EFDC-DS/EFDC-Explorer User Manual: 3D Hydrodynamic and water quality modelling system, Dynamic Solutions International, LLC, Knoxville, pp. 1-10.

Cruickshank, B., 2006. Modelling nutrient load to the Port Jackson estuary, Australia. B.Sc. Honours Thesis (unpubl), School of Geosciences, University of Sydney.

Das, P., Marchesiello, P., and Middleton, J. H., 2000. Numerical modelling of tide-induced residual circulation in Sydney Harbour. *Marine and Freshwater Research* 51, 97-112.

Davis, B. S., and Birch, G. F., in press. Investigation of runoff generation dynamics for a highly urbanised catchment based on manual picking of rainfall-runoff data. *J Hydrology*.

Etemad Shahidi, A., and Imberger, J., 2005. Vertical eddy diffusivity estimations in Swan River Estuary. *Dynamics of Atmospheres and Oceans*, 39(3-4), 175-187

Ferguson, C., Long, J., Simeoni, M., 1995. Stormwater monitoring report: 1994 Annual report, AWT Ensign report no. 95/94, prepared for the Clean Waterways Program, March 1995.

Galperin, B., L.H. Kantha., S. Hassid., and A. Rosati., 1988. A quasi-equilibrium turbulent energy model for geophysical flows. *Journal of Atmospheric Science* 45, 55-62.

Hamrick, J.M., 1992a. A Three Dimensional Environmental Fluid Dynamics Computer Code: Theoretical and Computational Aspects. The College of William and Mary, Virginia Institute of Marine Science. Special Report 317, 63 pp.

Hamrick, J. M., 1992b. Estuarine environmental impact assessment using a three-dimensional circulation and transport model. *Estuarine and Coastal Modelling, Proceedings of the 2nd International Conference*, M.L. Spaulding et al., Eds., American Society of Civil Engineers, New York, 292-303.

Hamrick, J. M., 1994a. Linking hydrodynamic and biogeochemical transport models for estuarine and coastal waters. *Estuarine and Coastal Modelling, Proceedings of the 3rd International Conference*, M.L. Spaulding et al., Eds., American Society of Civil Engineers, New York, 591-608.

Hatje V, Birch GF (2001a) Spatial and temporal variability of particulate trace metals in Port Jackson estuary, Australia. *Estuarine Coastal Shelf Science* 53, 63-77

Huang, W., and X. Liu., 2009. Effects of reducing river flow on pulse residence time in Little Manatee River, USA. *Transactions of Tianjin University* 15 (2), 95-100

Ji, Z. G., Morton, M. R., and Hamrick, J.M., 2000. Modelling Hydrodynamic and Sediment Processes in Morro Bay, *Estuarine and Coastal Modelling: Proceedings, 6th International Conference.*, M.L. Spaulding and H. L. Butler, Eds., American Society of Civil Engineers, New York, 1035-1054.

Jin, K. R., J.M. Hamrick., and T. Tisdale., 2000. Application of a Three-Dimensional Hydrodynamic Model for Lake Okeechobee, *Journal of Hydraulic Engineering*, 126 (10), 758-771.

Kuo, A.Y., Shen, J., and Hamrick J.M., 1996. The Effect of Acceleration on Bottom Shear Stress in Tidal Estuaries. *Journal of Waterway, Port, Coastal and Ocean Engineering*. ASCE, 122 (2). 75-83.

- Lin, J., Kuo, A.Y., 2003. A model study of turbidity maxima in the York River estuary, Virginia. *Estuaries* 26 (5), 1269-1280
- Lin, L., L. Xie., L.J. Pietrafesa., J.S. Ramus and H.W. Paerl., 2007. Water quality gradients across Albemarle-Pamlico Estuarine system: seasonal variations and model applications, *Journal of Coastal Research* 23 (1), 213-229
- Lin, J., L. Xie, L.J., Pietrafesa, H. Xu., W. Woods., M.A. Mallin and M.J Durako., 2008a, Water quality responses to simulated flow and nutrient reductions in the Cape Fear River Estuary and adjacent coastal region, North Carolina, *Ecological Modelling*, 212, 200-217.
- Liu, X., and Huang,W., 2009. Modelling sediment resuspension and transport induced by storm wind in Apalachicola Bay, USA. *Environmental Modelling & Software* 24, 1302-1313
- Liu, Z., N.B. Hashim., W.L. Kingery., D.H. Huddleston., M. Xia., 2008. Hydrodynamic modelling of St Louis Bay estuary and watershed using EFDC and HSPF. *Journal of Coastal Research* 52, 107-116
- Luo, F., and R. Li., 2009. 3D Water environment simulation for North Jiangsu offshore Sea based on EFDC, *Journal of Water Resource and Protection* 1, 41-47
- McLoughlin, L.C., 2000a. Shaping Sydney Harbour: sedimentation, dredging and reclamation 1788-1990's'. *Australian Geographer* 31 (2), 183-208.
- Moustafa, M.Z., & J.M. Hamrick., 1994. Modelling circulation and salinity transport in the Indian River Lagoon. *Estuarine and Coastal Modelling Proceedings of the 3rd International Conference*, M.L. Spaulding et al., Eds., American Society of Civil Engineers, New York, 381-395
- Park, K., Jung, H. S., Kim, H. S., and Ahn, S., 2005. Three-dimensional hydrodynamic eutrophication model (HEM-3D): application to Kwang-Yang Bay, Korea, *Marine Environmental Research* 60, 171-193

Rochford, L., 2008. Stormwater heavy metal loading to Port Jackson estuary, NSW, Australia. M.Sc. Thesis (unpubl) School of Geosciences, University of Sydney.

Roy, P., 1983, Quaternary Geology. In Geology of the Sydney 1:100,000 Sheet. Ed. C. Herbert. Publ. Geological Survey of NSW, Dept. of Mineral Resources, Sydney, Australia

Schlesinger, W.H., 1997. Biogeochemistry: an analysis of global change. Academic Press, San Diego, CA, 588pp.

Shen, J., and A.Y. Kuo., 1999. Numerical Investigation of an estuarine front and it's associated topographic eddy. Journal of Waterway, Port, Coastal and Ocean Engineering 125, 127-135

Shen, J., Boon., J., and Kuo, A.Y., 1999a, A Numerical Study of a Tidal Intrusion Front and Its Impact on Larval Dispersion in the James River Estuary, Virginia, Estuaries 22 (3), 681-692.

Shen, J., and L. Haas., 2004. Calculating age and residence time in the tidal York River using three-dimensional model experiments. Estuarine, Coastal Shelf Science 61, 449-461.

Shen, J., Lin, J., 2006. Modelling study of the influences of tide and stratification on age of water in the tidal James River, Estuarine, Coastal and Shelf Science 68 (1-2), 101-112.

Smagorinski, J., 1963. General circulation experiments with the primitive equations, Part I: The basic experiment. Monthly Weather Review 91, 99-152

Taylor, S.E., 2000. The source and remobilisation of contaminated sediment in Port Jackson, Australia. PhD thesis, Division of Geology and Geophysics, School of Geosciences, University of Sydney, Australia.

Telydyne RD Instruments., 2007. WinRiver II User's Manual.

Tetra Tech., 1999. Theoretical and Computational Aspects of Sediment Transport in the EFDC Model, Technical Report Prepared for U.S. Environmental Protection Agency, Tetra Tech, Inc., Fairfax, Va.

Tuckey, B.J., Gibbs, M. T., Knight, B. R., and Gillespie, P. A., 2006. Tidal circulation in Tasman and Golden Bays: Implications for river plume behaviour, New Zealand Journal of Marine and Freshwater Research 40 (2), 305-324

Wolanski, E., 1977. The fate of storm water and stormwater pollution in the Parramatta Estuary, Sydney. Australian Journal of Marine and Freshwater Research 28, 67-78

Xu, H., Lin, J., and Wang, D., 2008. Numerical study on salinity stratification in the Palmico River estuary. Estuarine, Coastal and Shelf Science 80, 74-84

Yang, Z., 1996. Variational inverse methods for transport problems. Ph.D. dissertation the College of William and Mary, Williamsburg, VA.

Zarilo, G.A., and Surak, C.R., 1995. Evaluation of submerged reef performance at Vero Beach, Florida, using a numerical modelling scheme. A report to Indian River County Florida. Florida Institute of Technology, 56pp.

Zarillo, G.A. 1998, Application of a three-dimensional model to evaluate improvements in the Long Slip Canal entrance basin in the Hudson River. Dames and Moore, Inc., 58pp.

Figure 1. Site map of the Sydney Estuary and surrounding catchment, depicting the major tributaries, estuary regions and rainfall gauge locations

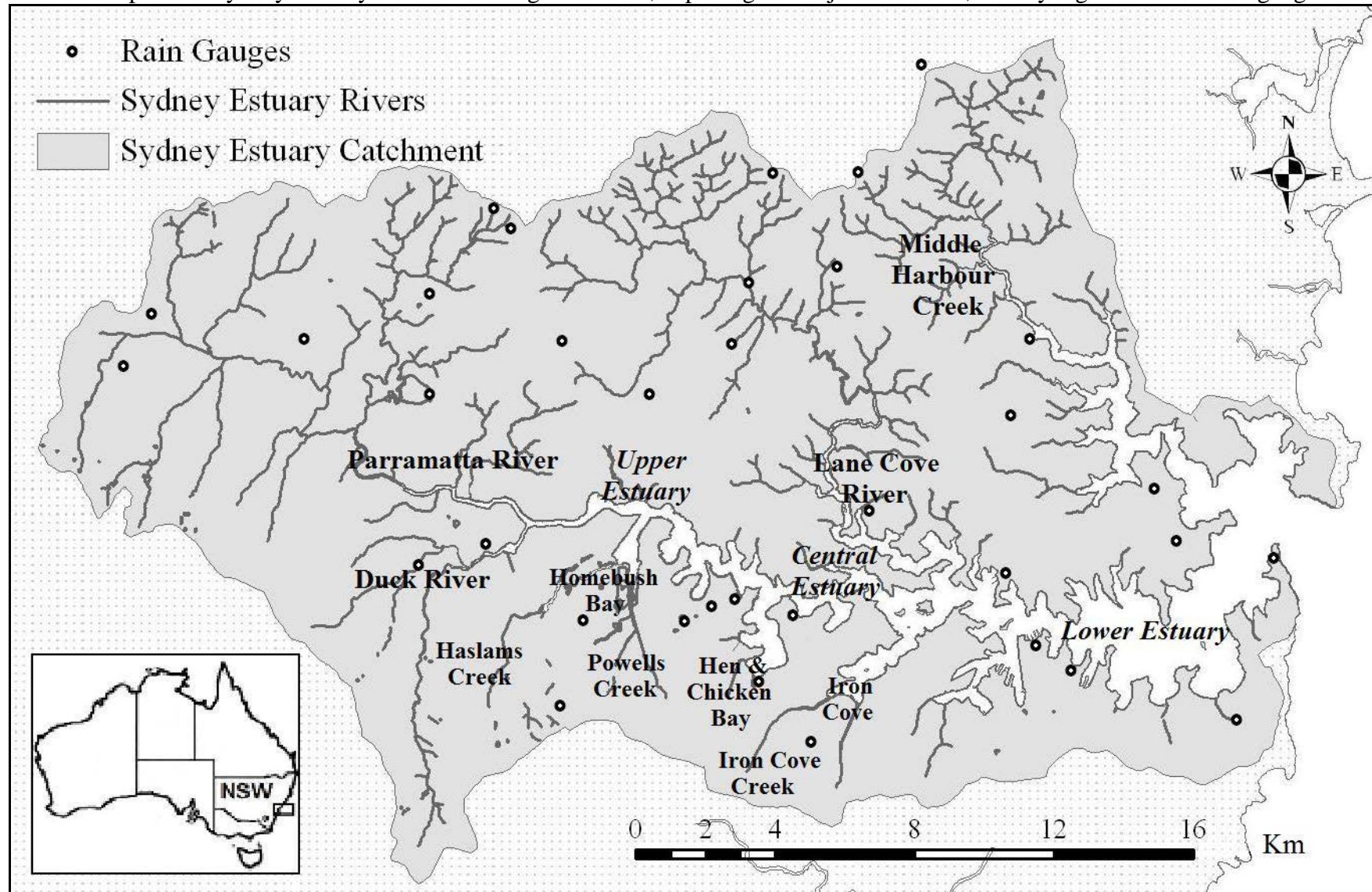


Figure 2a. The Sydney Estuary field site locations including ADCP transects (T₁–T₉).

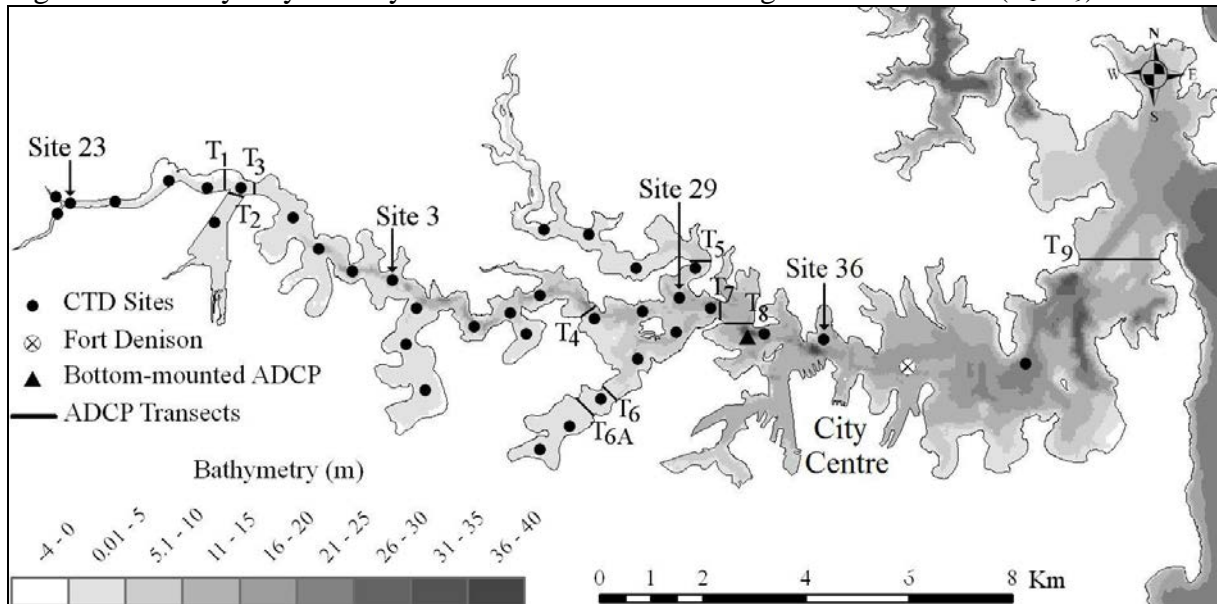


Figure 2b. A course version of the Sydney Estuary model grid. The grid used in the present study is based upon that shown but has a higher resolution than that displayed (~12000 cells as opposed to ~ 2500 cells). Inset - Regions displayed in light grey represent the 19 subcatchments for which runoff coefficient data were available.

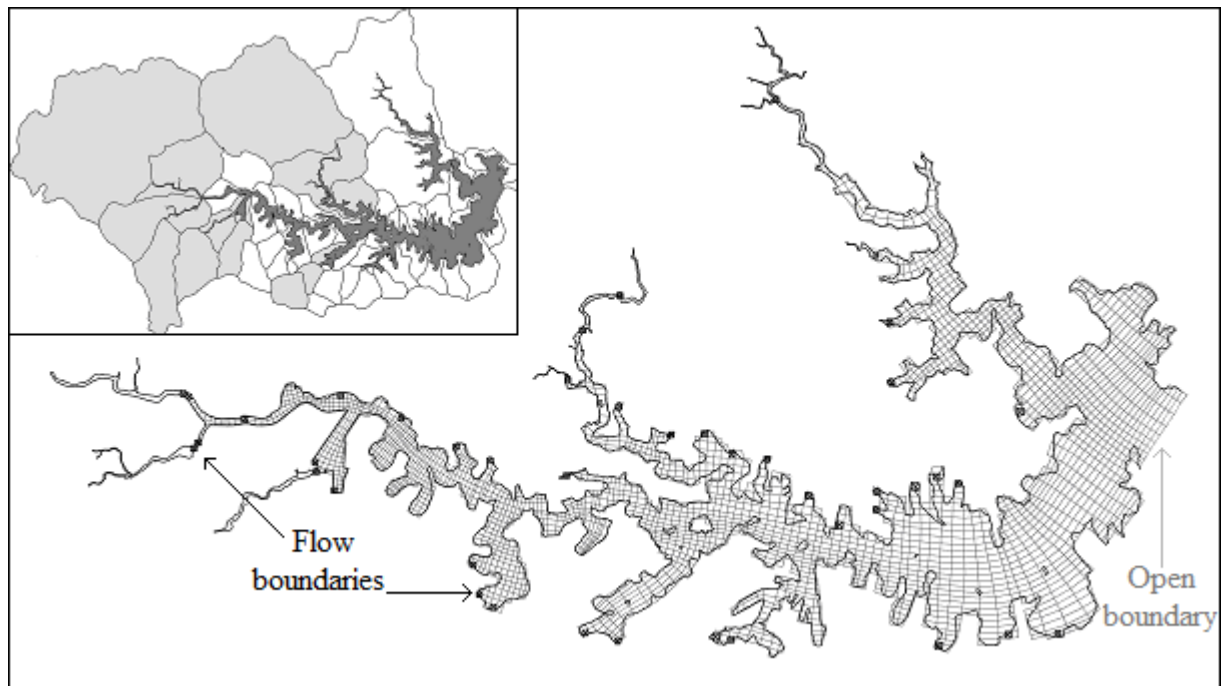


Figure 2c. Wind data for the rain event and subsequent field monitoring period, recorded every 30 minutes at Fort Denison (see Figure 2a.) in the lower Sydney estuary. Direction is reported as the direction the wind is blowing from.

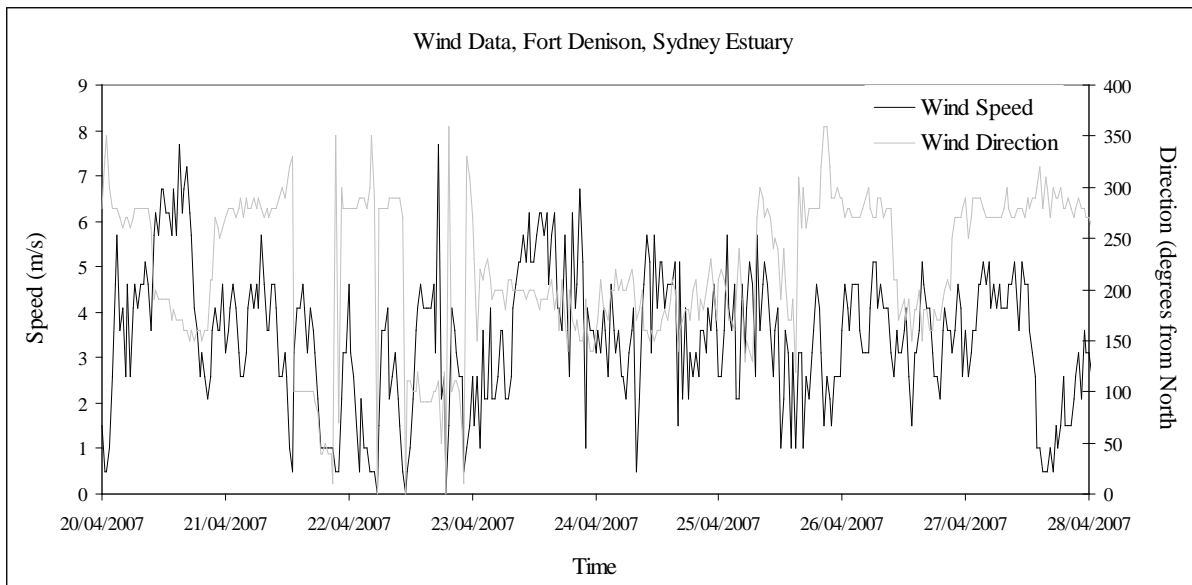


Figure 3a. Measured and predicted water level at Fort Denison.

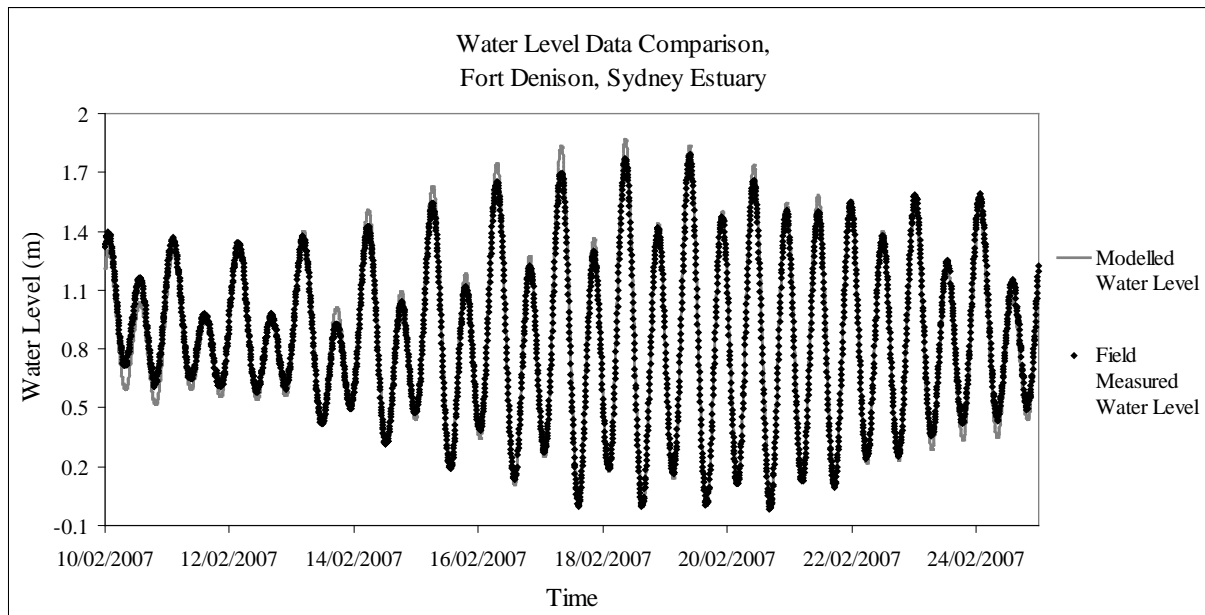


Figure 3b. Comparison of discharge data

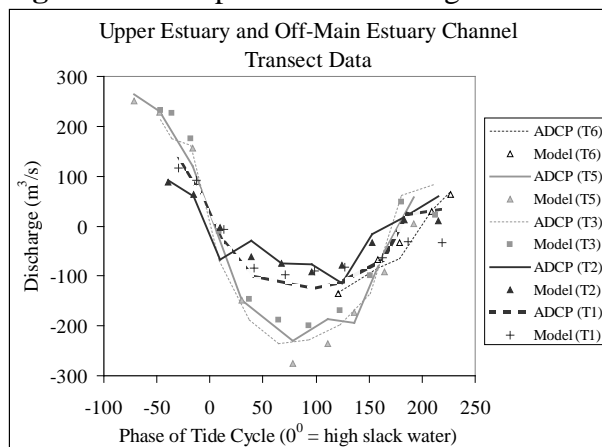


Figure 3c. Comparison of discharge data

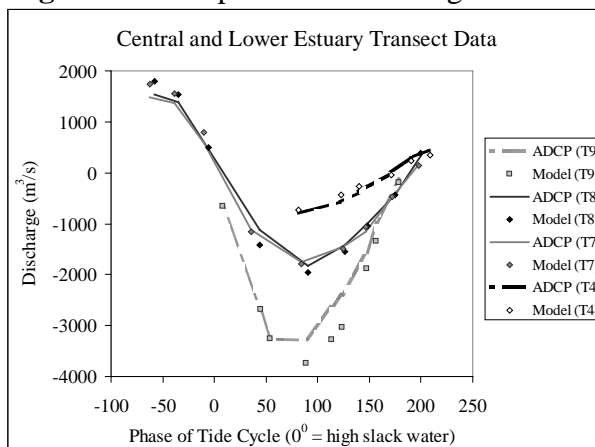


Figure 3d. Comparison of measured (bottom-mounted ADCP, Figure 2) and predicted current speed at Balls Head.

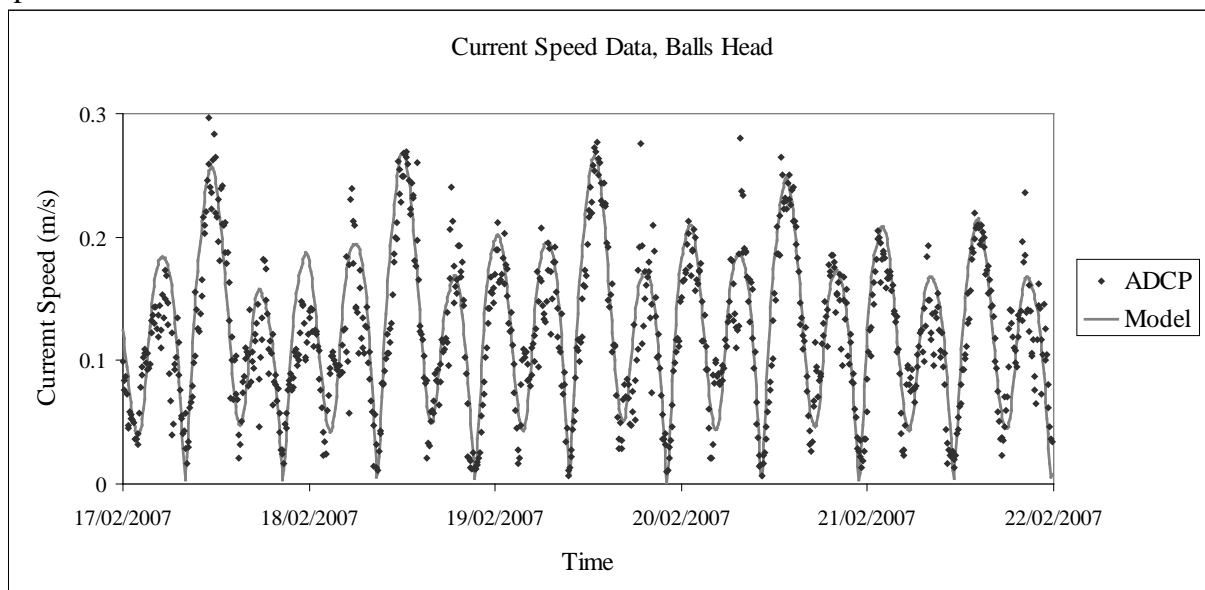


Figure 3e. Measured and predicted current speeds across Transect 9 at mid-ebb tide.

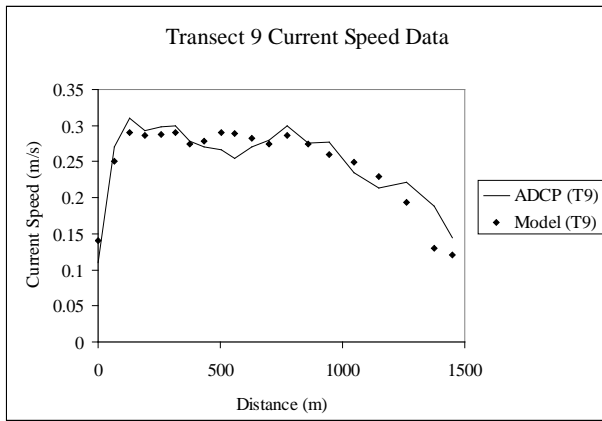


Figure 3f. Measured and predicted current speeds across Transect 2 and 7 at mid-ebb tide.

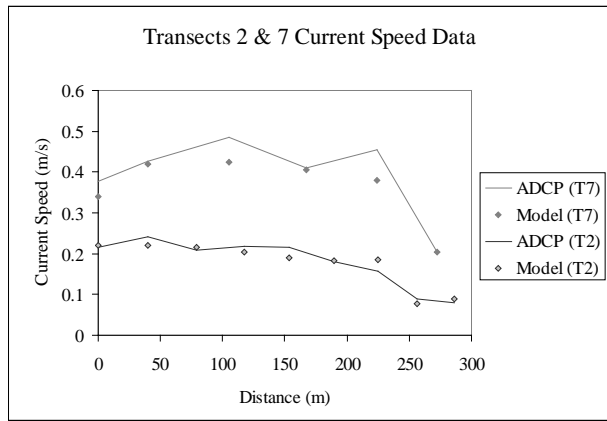
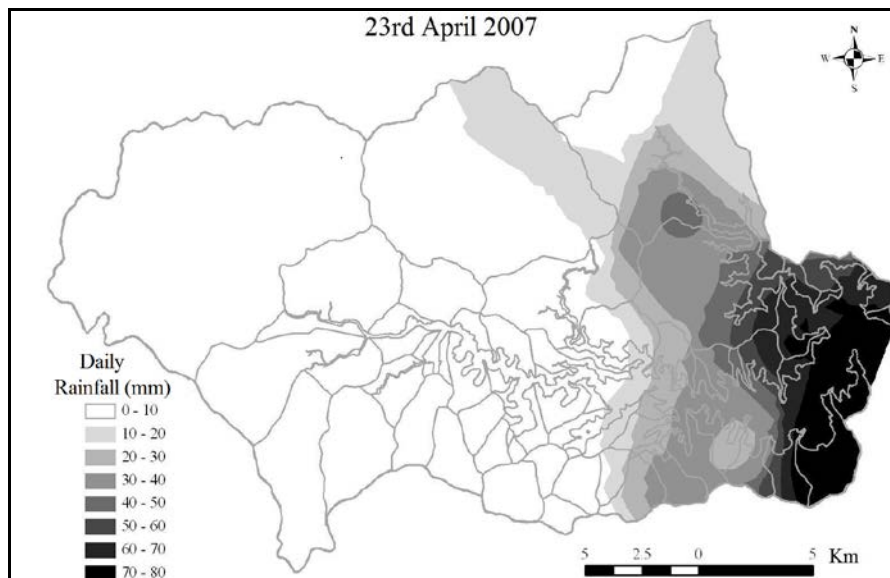
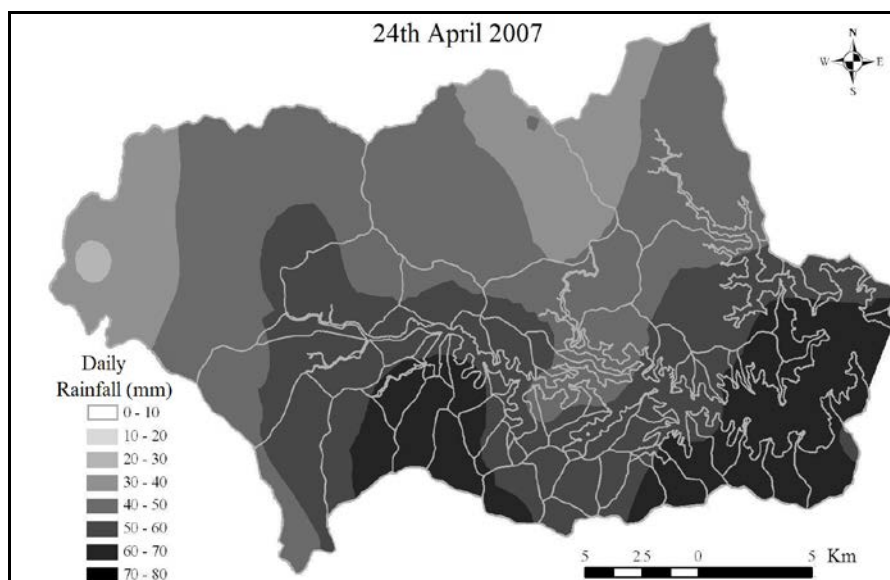


Figure 4. Rainfall Distribution across the Sydney Catchment, April 2007

4a.



4b.



4c.

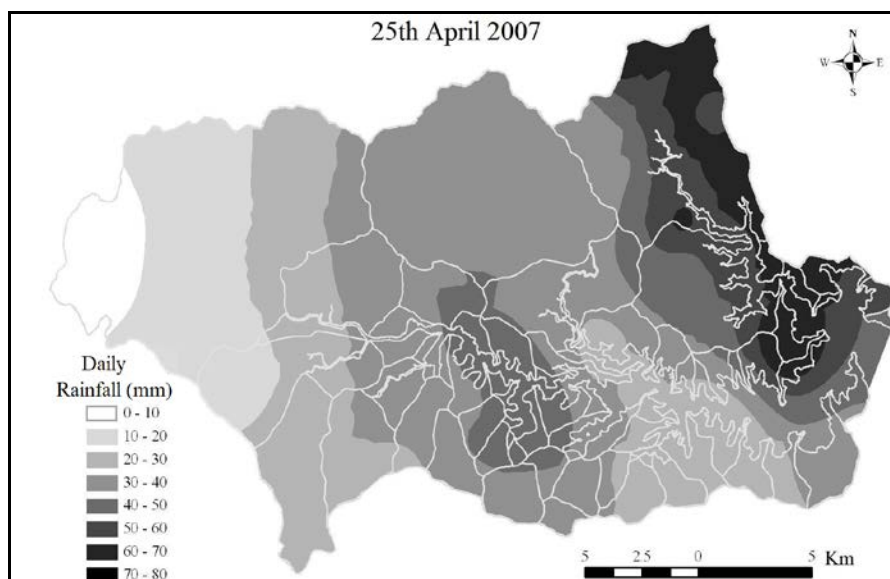
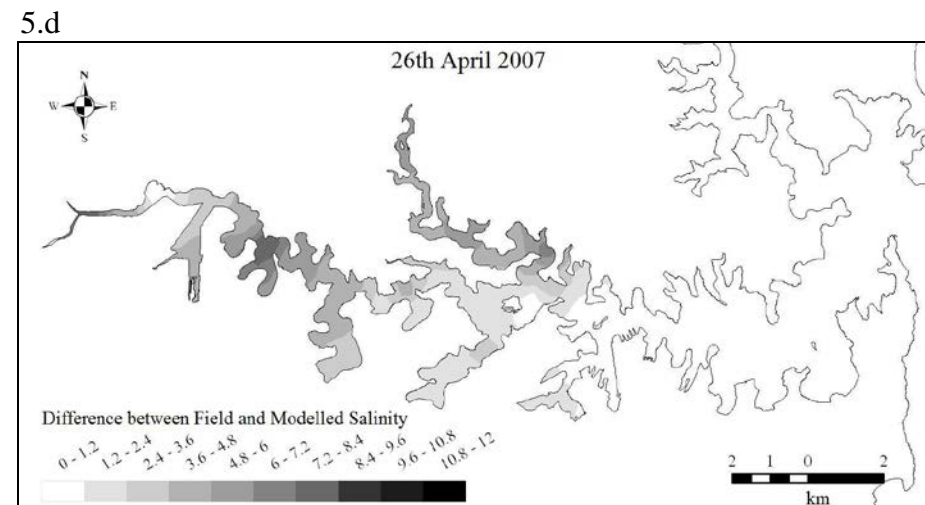
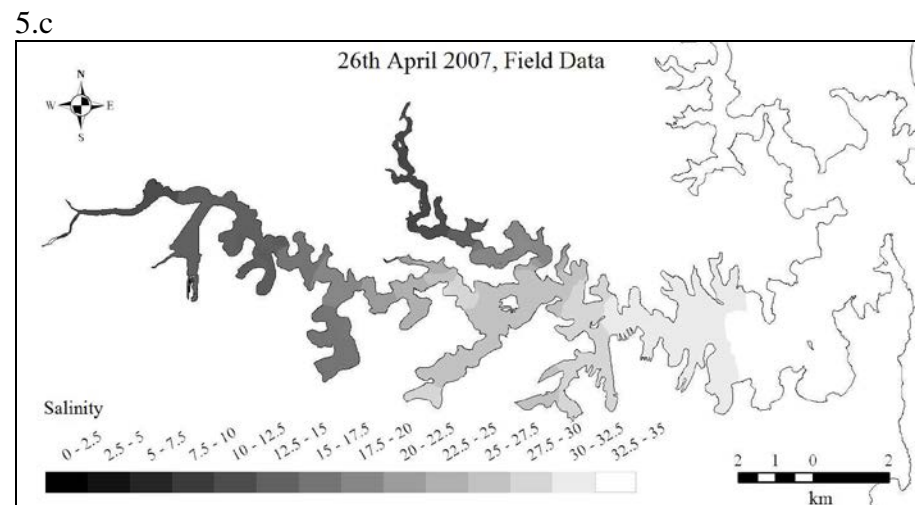
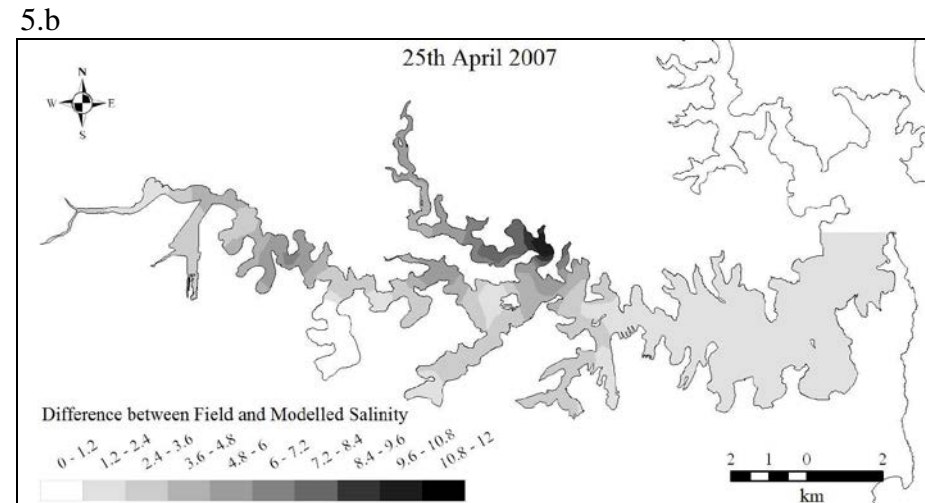
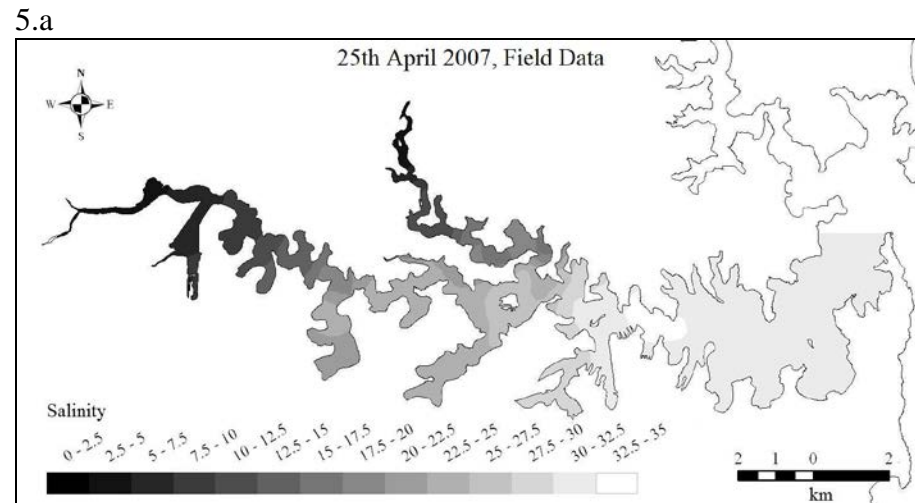
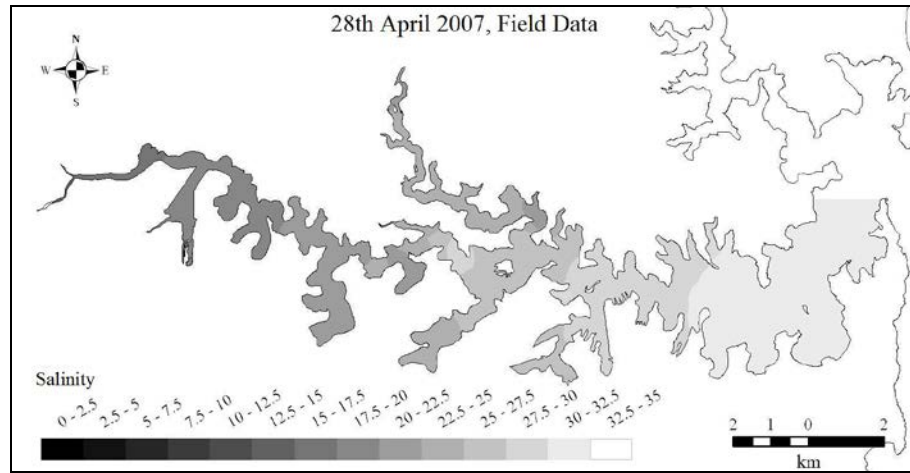


Figure 5. Surface-water salinity maps generated from field data measured 0.5m below the waters surface (5a, 5c and 5e) and corresponding maps of the difference between measured and modelled salinity 0.5m below the waters surface (5b, 5d and 5f).



5.e



5.f

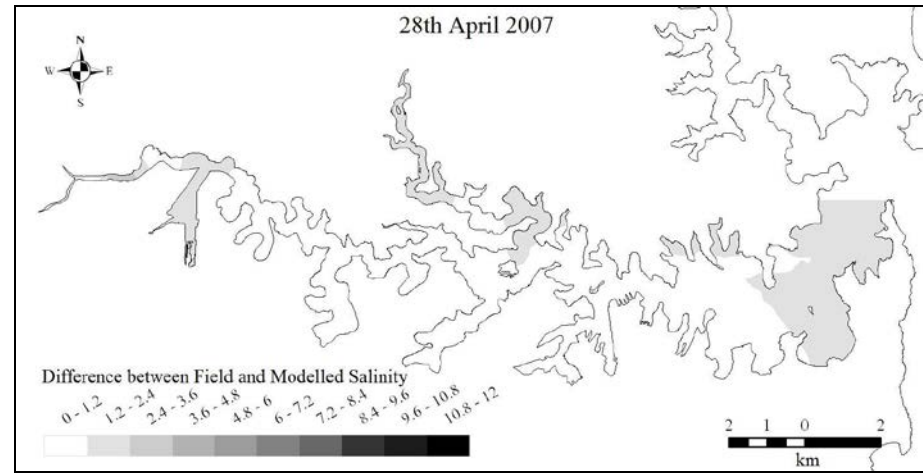
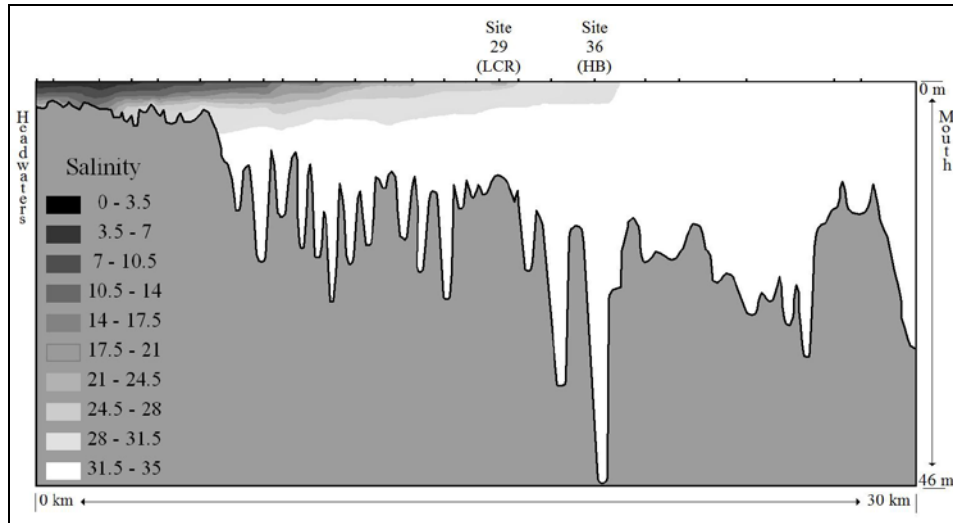
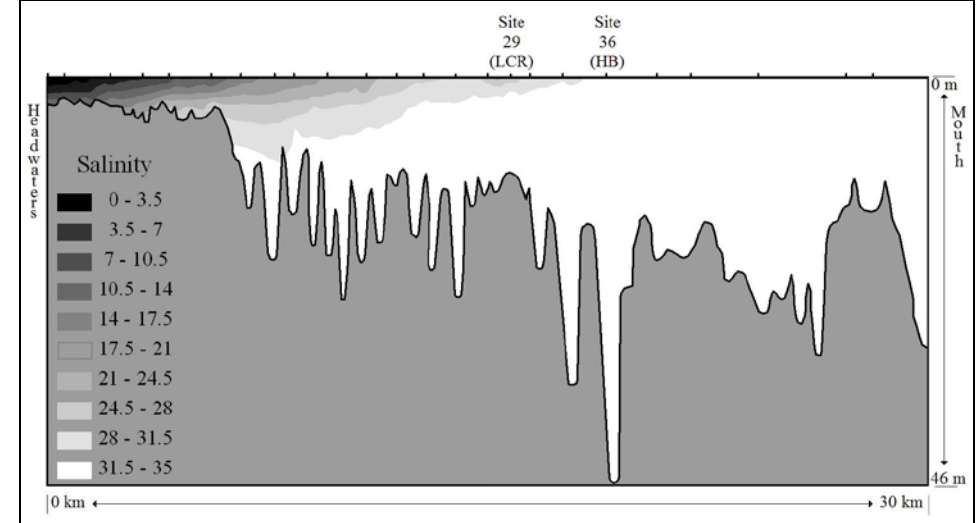


Figure 6. Profiles along the axis of the main channel representing field (6a, 6c and 6e) and model-predicted (6b, 6d, 6f, 6g, 6h and 6i) salinity distributions from the headwaters to the estuary mouth. Site 29 (LRC) is where the Lane Cove River joins the main channel. Site 36 (HB) is near the Sydney Harbour Bridge.

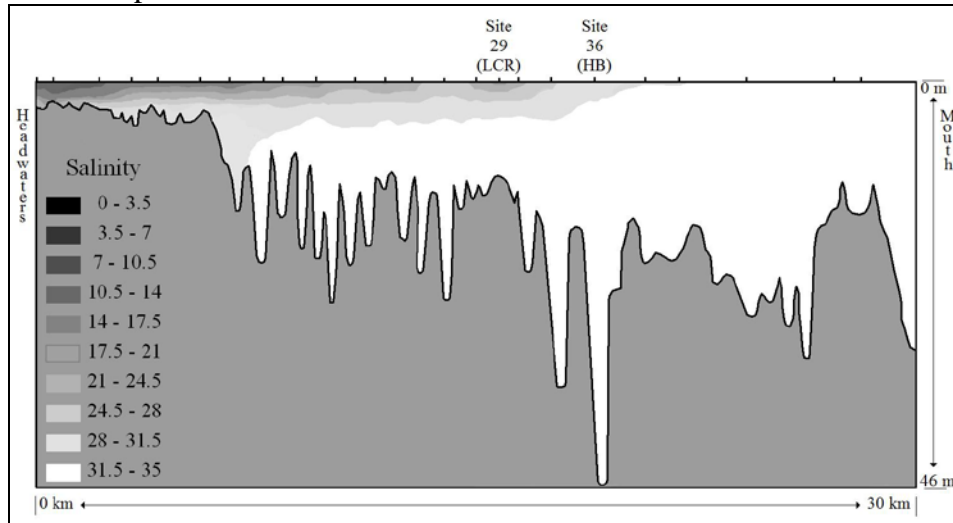
6.a 25th April 2007 field results



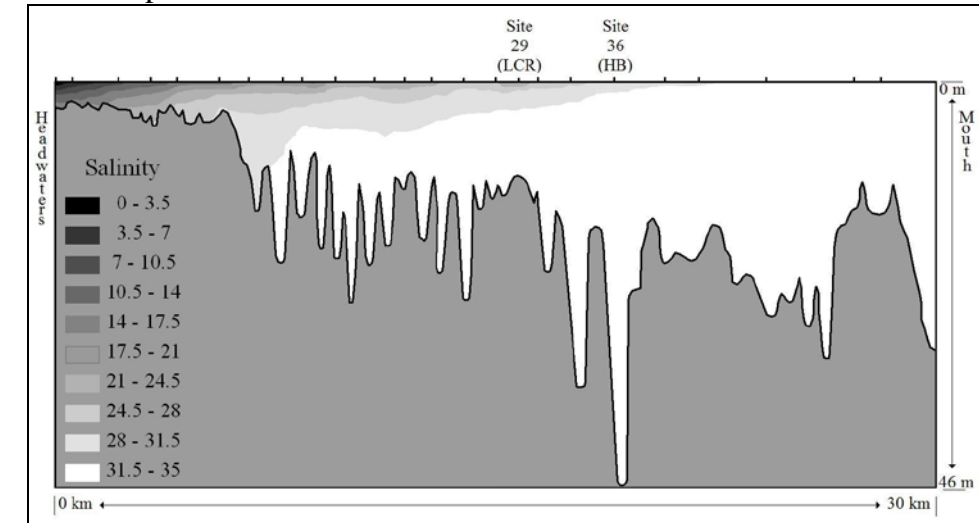
6.b 25th April 2007 model results



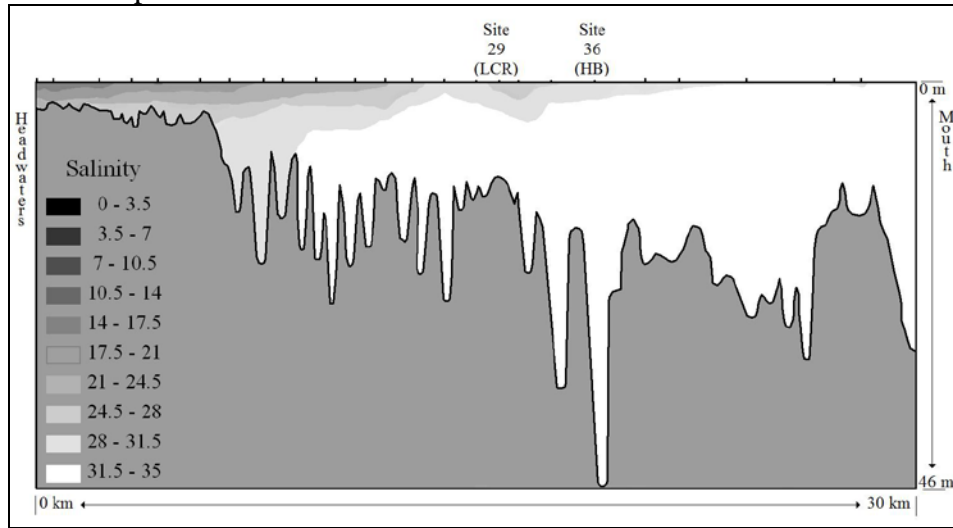
6.c 26th April 2007 field results



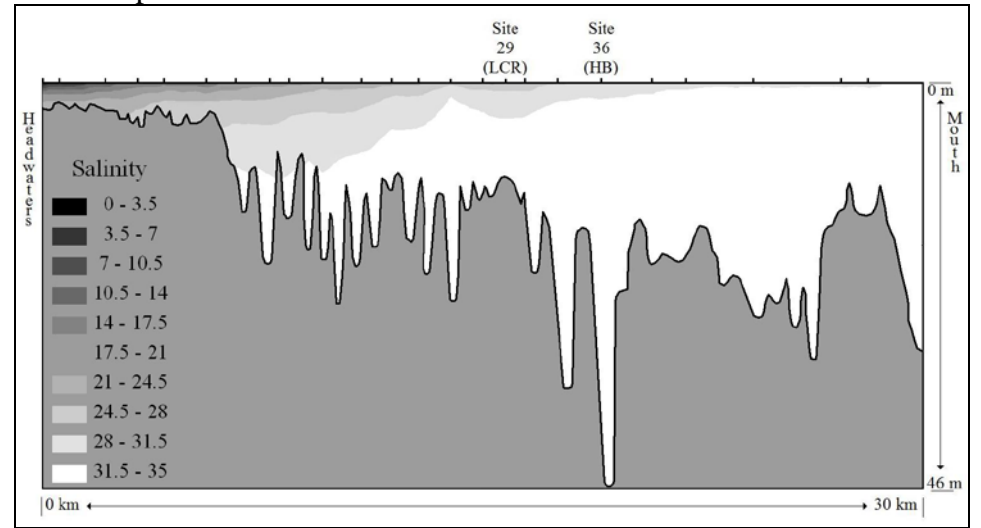
6.d 26th April 2007 model results



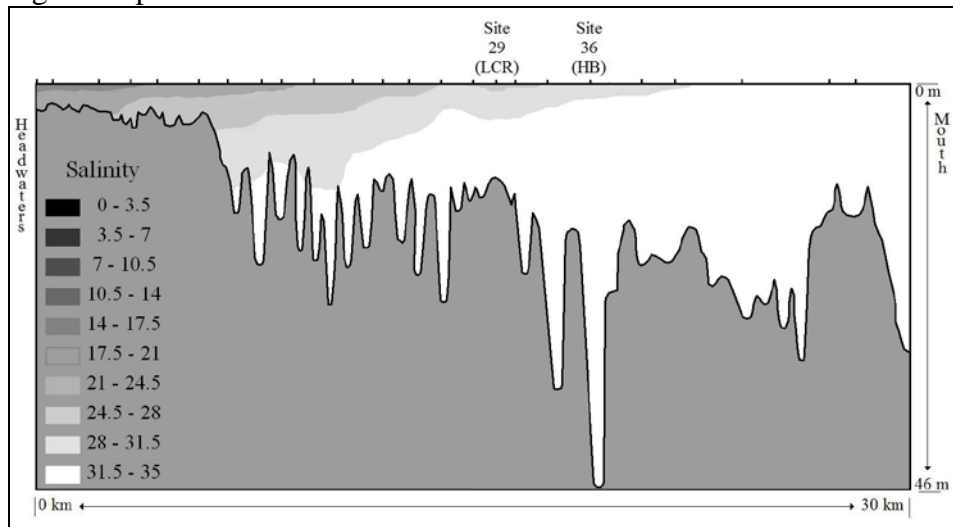
6.e 28th April 2007 field results



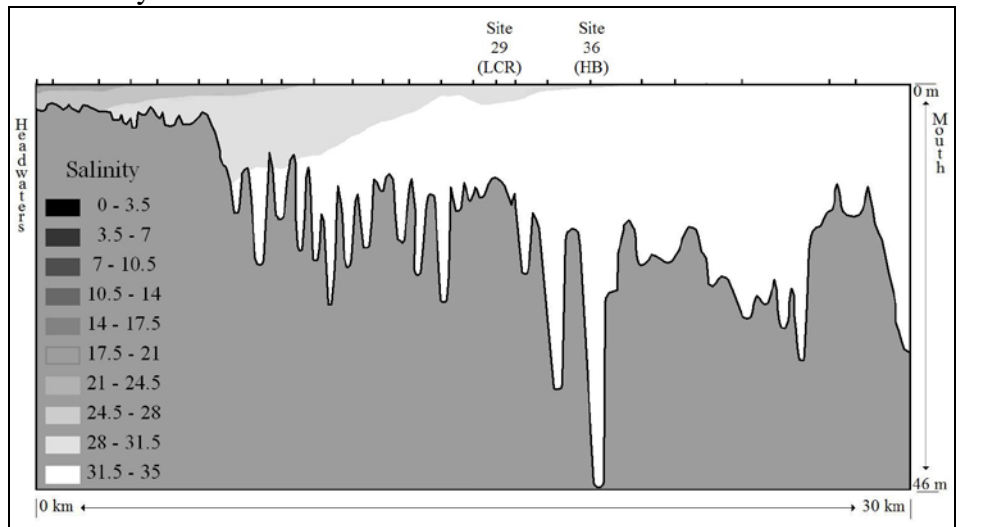
6.f 28th April 2007 model results



6.g 30th April 2007 model results



6.h 7th May 2007 model results



6.i 15th May 2007 model results

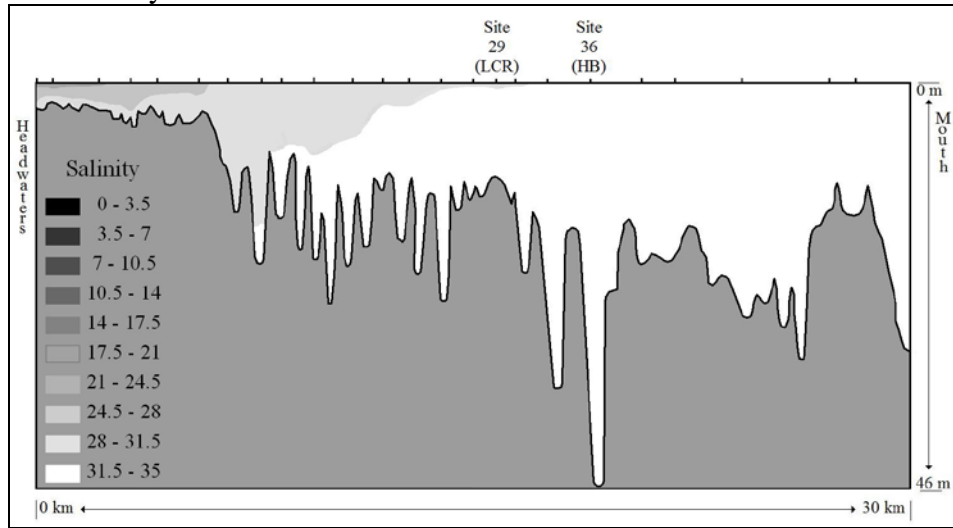
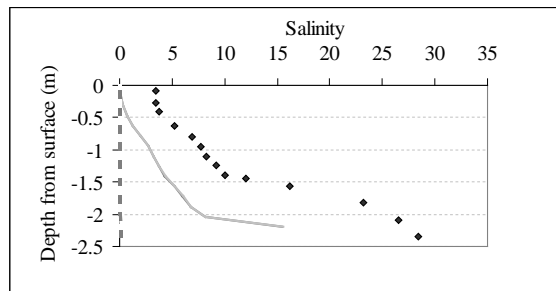


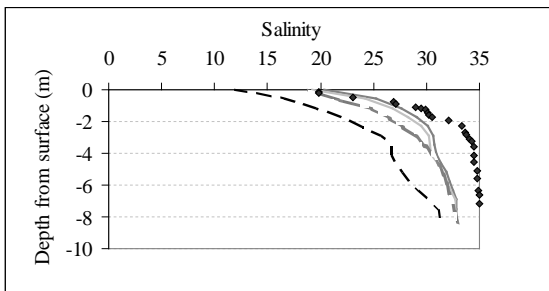
Figure 7. Field and modelled vertical salinity profiles from three different estuary sites (Sites 23, 3 and 29 displayed in Figure 2a.). Model results show vertical salinity profiles predicted by the four different runoff scenarios.

7a. 25th April 2007

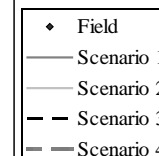
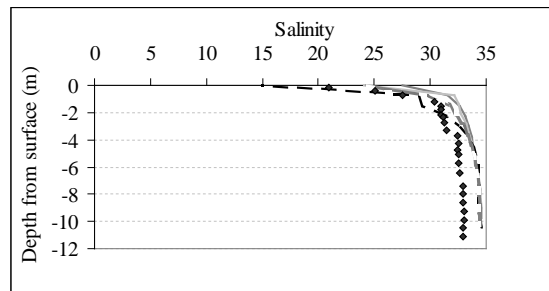
Site 23



Site 3

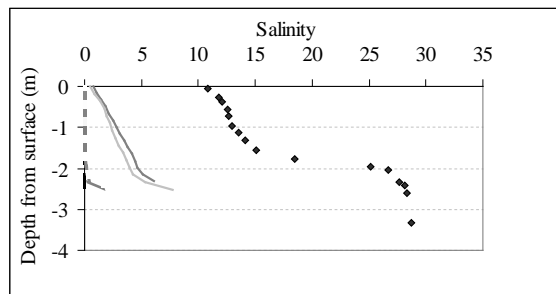


Site 29

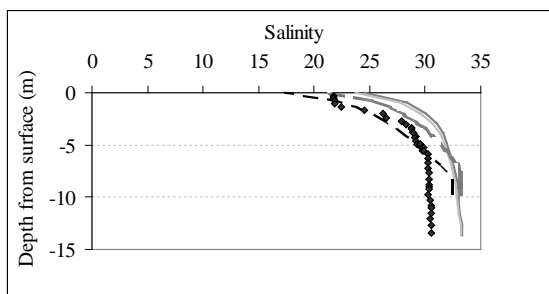


7b. 26th April 2007

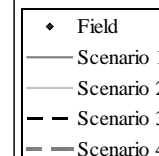
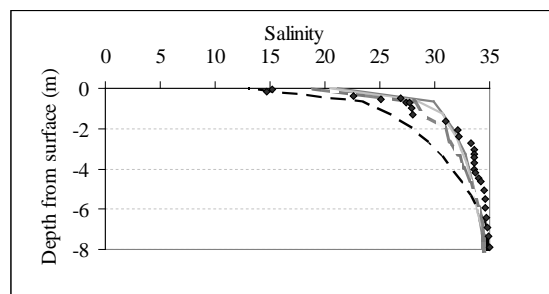
Site 23



Site 3

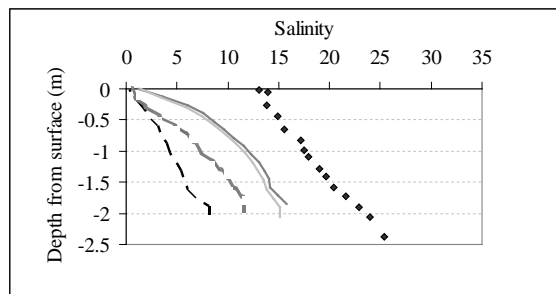


Site 29

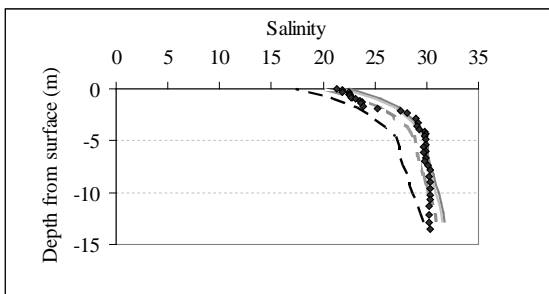


7c. 28th April 2007

Site 23



Site 3



Site 29

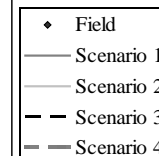
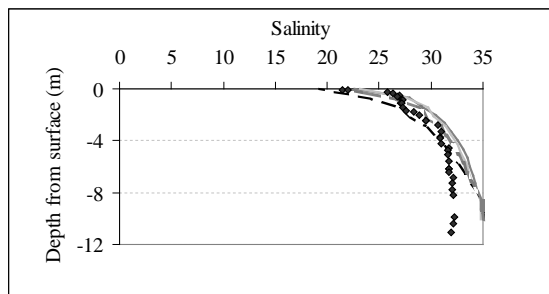


Table 1. Agreement between field-measured and modelled current speed data sets.

Transect	T2	T3	T5	T6	T7	T8	T9
Correlation (r^2) between measured and modelled current speed data	0.8	0.89	0.72	0.44	0.95	0.9	0.82
RMSE (cm/s)	2.5	3.2	3.7	2.5	3.5	3.4	3.3
Av Difference between measured and modelled current speed (cm/s)	1.9	2.2	2.9	2	2.8	2.3	2.6
Max Difference between measured and modelled current speed (cm/s)	6.6	10	9.2	8.2	9	9.8	10

Table 2. Agreement between field-measured and modelled salinity data sets

	Scenario 1	Scenario 2	Scenario 3	Scenario 4
RMSE	3.3	3.3	6.2	4.6
% (Modelled salinity - measured salinity) < 5 PSU	85.50%	89.20%	68.10%	82.60%
% (Modelled salinity - measured salinity) > 5 PSU	14.50%	10.80%	31.90%	17.40%
% (Modelled salinity - measured salinity) > 10 PSU	1.80%	1.20%	10.70%	5.30%
% (Modelled salinity - measured salinity) > 15 PSU	0.40%	0%	3.30%	1.20%

Figure Captions

Figure 1. Site map of the Sydney Estuary and surrounding catchment, depicting the major tributaries, estuary regions and rainfall gauge locations.

Figure 2a. The Sydney Estuary field site locations including ADCP transects (T₁–T₉).

Figure 2b. A course version of the Sydney estuary model grid. The grid utilised in modelling studies has a higher resolution than that displayed (~12000 cells as opposed to ~2500 cells) and is based upon that displayed. Inset - Regions displayed in light grey represent the 19 subcatchments for which runoff coefficient data were available.

Figure 2c. Wind data for the rain event and subsequent field monitoring period, recorded every 30 minutes at Fort Denison (see Figure 2a.) in the lower Sydney estuary. Direction is reported as the direction the wind is blowing from.

Figure 3a. Measured and predicted water level at Fort Denison.

Figure 3b. Comparison of discharge data

Figure 3c. Comparison of discharge data

Figure 3d. Comparison of measured (bottom-mounted ADCP, Figure 2) and predicted current speed at Balls Head

Figure 3e. Measured and predicted current speeds across Transcet 9 at mid-ebb tide.

Figure 3f. Measured and predicted current speeds across Transect 2 and Transect 7 at mid-ebb tide.

Figure 4. Rainfall Distribution across the Sydney Catchment, April 2007

Figure 5. Surface-water salinity maps generated from field data measured 0.5m below the waters surface (5a, 5c and 5e) and corresponding maps of the difference between measured and modelled salinity 0.5m below the waters surface (5b, 5d and 5f).

Figure 6. Profiles along the axis of the main channel representing field (6a, 6c and 6e) and model-predicted (6b, 6d, 6f, 6g, 6h and 6i) salinity distributions from the headwaters to the estuary mouth. Site 29 (LRC) is where the Lane Cove River joins the main channel. Site 36 (HB) is near the Sydney Harbour Bridge.

Figure 7. Field and modelled vertical salinity profiles from three different estuary sites (Sites 23, 3 and 29 displayed in Figure 2a.). Model results show vertical salinity profiles predicted by the four different runoff scenarios.

7a. 25th April 2007

7b. 26th April 2007

7c. 28th April 2007

Table Captions

Table 1. Agreement between field and modelled current speed data.

Table 2. Agreement between field and modelled salinity data